Chinese Physical Society | IOP Publishing
CPB
Chinese Physics B
http://cpb.iphy.ac.cn https://iopscience.iop.org/journal/1674-1056

Magnetic van der Waals materials: Synthesis, structure, magnetism, and their potential applications

Zhongchong Lin(林中冲), Yuxuan Peng(彭宇轩), Baochun Wu(吴葆春), Changsheng Wang(王常生), Zhaochu Luo(罗昭初), and Jinbo Yang(杨金波)

Citation: Chin. Phys. B, 2022, 31 (**8**): 087506. DOI: 10.1088/1674-1056/ac6eed
Journal homepage: http://cpb.iphy.ac.cn; http://iopscience.iop.org/cpb

Chin. Phys. B **31**, 087506 (2022)

TOPICAL REVIEW — Celebrating 30 Years of *Chinese Physics B*

Magnetic van der Waals materials: Synthesis, structure, magnetism, and their potential applications

Zhongchong Lin(林中冲)[1,2], Yuxuan Peng(彭宇轩)[1,2], Baochun Wu(吴葆春)[1,2], Changsheng Wang(王常生)[1,2,3], Zhaochu Luo(罗昭初)[1,2,†], and Jinbo Yang(杨金波)[1,2,3,4,5,‡]

[1] *State Key Laboratory for Mesoscopic Physics, School of Physics, Peking University, Beijing* 100871, *China*
[2] *Institute of Condensed Matter Physics and Materials, School of Physics, Peking University, Beijing* 100871, *China*
[3] *Beijing Key Laboratory for Magnetoelectric Materials and Devices, Beijing* 100871, *China*
[4] *Collaborative Innovation Center of Quantum Matter, Beijing* 100871, *China*
[5] *Peking University Yangtze Delta Institute of Optoelectronics, Nantong* 226010, *China*

(Received 12 April 2022; revised manuscript received 9 May 2022; accepted manuscript online 12 May 2022)

As the family of magnetic materials is rapidly growing, two-dimensional (2D) van der Waals (vdW) magnets have attracted increasing attention as a platform to explore fundamental physical problems of magnetism and their potential applications. This paper reviews the recent progress on emergent vdW magnetic compounds and their potential applications in devices. First, we summarize the current vdW magnetic materials and their synthetic methods. Then, we focus on their structure and the modulation of magnetic properties by analyzing the representative vdW magnetic materials with different magnetic structures. In addition, we pay attention to the heterostructures of vdW magnetic materials, which are expected to produce revolutionary applications of magnetism-related devices. To motivate the researchers in this area, we finally provide the challenges and outlook on 2D vdW magnetism.

Keywords: van der Waals magnetic materials, 2D magnetism, modulation methods, spintronics

PACS: 75.50.−y, 85.75.−d, 75.70.Cn **DOI:** 10.1088/1674-1056/ac6eed

1. Introduction

Magnetism, records of which date back to the magic attraction of lodestones to iron nearly 3000 years ago, is a fundamental property of matter.[1–3] The magnetically ordered state is of great significance to develop technologies and achieve applications, including electric generators,[4–7] magneto-optics devices,[3,8] and magnetic logic and memory devices.[9,10] Two-dimensional (2D) van der Waals (vdW) materials have naturally layered structures and highly crystalline characteristics[11] with exotic phenomena, such as tunable bandgap,[12–14] high carrier mobility,[15,16] and linear dichroism.[9,17] In addition, few-layer vdW materials are sensitive to external stimuli. Thus, vdW materials provide an opportunity to control various physical properties such as electrical, optical, and magnetic properties.[11,18,19] In strong contrast to the electrical and optical properties, which have been intensively studied and reviewed, intrinsic magnetism of 2D vdW materials was not discovered until recent years.[20–22]

The timeline of milestone discoveries/events in 2D magnetism can be roughly divided into three stages dated from the 1940s (see Fig. 1).[23] In 1944, Onsager *et al.*[24] speculated that a monolayer-thick Ising-type magnet possessed a stable long-range magnetic order. Subsequently, the Mermin–Wagner theorem demonstrated that long-range magnetic order is forbidden in the 2D isotropic Heisenberg-type magnet.[25] The quasi-2D magnetism was identified and found in some magnets, such as K_2NiF_4, where weak or non-interacting interlayer exchange coupling prevents magnetic order in the third dimension.[26,27] During the second stage, from the 1970s to the 1990s, atomically thin magnetic films emerged, and the Ising model was verified.[28–30] However, magnetic films are pseudo-2D magnets without 2D nature due to the dangling bonds at the surface and substrate influences on lattice match and electronic distribution.[30–32] The third stage started with the discovery of graphene in 2004.[33] The family of 2D vdW materials has been growing, and a series of novel physical phenomena have been continuously revealed.[34,35] The 2D vdW magnetic materials remained a conspicuously missing member of this family in the decade. During this period, defect engineering, including vacancies, adatoms, boundaries, and edges, was adapted to induce magnetism in non-magnetic vdW materials,[11,36] for instance, the point-defect pyrolytic graphite and $PtSe_2$,[37,38] nitrogen-doped graphene,[39] carbon-doped BN nanosheets,[40,41] and zigzag-edge graphene.[42] However, the extrinsically induced magnetic response is somewhat susceptible, fairly weak, short-ranged, and unstable. Until 2016, antiferromagnetism (AFM) was found in monolayer vdW $FePS_3$.[43,44] Subsequently, intrinsic ferromagnetism (FM) in monolayer CrI_3 and bilayer $Cr_2Ge_2Te_6$ vdW magnets was discovered in 2017,[20,21] un-

†Corresponding author. E-mail: zhaochu.luo@pku.edu.cn
‡Corresponding author. E-mail: jbyang@pku.edu.cn

 http://iopscience.iop.org/cpb http://cpb.iphy.ac.cn

veiling a new species of vdW materials. Magnetic anisotropy, which opens a gap in the spin-wave spectrum to resist the thermal fluctuations, enables FM ordering in Heisenberg-type bilayer $Cr_2Ge_2Te_6$,[45] which is different from the situation of the Ising-type magnets CrI_3. After these prior works, many other vdW magnetic materials have been discovered and investigated in the last five years.[20,21,46] The progress in the field of vdW magnetic materials involves three main directions.

1. Exploration of new vdW magnetic materials The vdW magnetic materials have attracted great attention, but the current vdW magnetic family is still far from meeting the demand of practical applications. To date, many unexplored candidates based on theoretical predictions require specialized growth techniques to synthetize. Thus, exploring more novel vdW magnetic compounds has been a major research direction in the magnetism/spintronics and 2D vdW materials communities, which is expected to yield an enriched landscape of emergent phenomena and unanticipated applications.

2. Fundamental issues of condensed matter physics Both the spin dimension and the spatial dimension are decisive factors in determining low-dimensional magnetism. The vdW magnetic materials provide an ideal platform to study the Hamiltonians of the fundamental magnetism models including the Ising, XY, and Heisenberg models.[23] Besides, novel quantum phases can be observed and studied, such as spin-valley coupling, magnetic excitons and magneto-optical effect, which are challenging and worthy of work.[34,47] The realization of quantum and topological phases is also exciting. One typical example is quantum spin liquids originated from Kitaev exchange interaction under 2D honeycomb lattice, which is likely to offer a strategy for magnetic Majorana fermions.[48–51]

3. Device applications of vdW magnetic materials Magnetic properties of atomically thin vdW magnets are susceptible to being manipulated by electrical ways, which is the central topic in spintronics. Besides, with the advantages of atomically flat surfaces, no dangling bonds and vdW heterostructures, vdW magnets are expected to realizes a series of spin-related devices including spin valves, spin–orbit torque, spin field-effect transistors, spin-filter, magnetic tunnel junctions, etc.[11,22,31]

As a vibrant and rapidly progressing field, it is worth summarizing the recent advancements in magnetism of the vdW family and its emerging applications which are the main scope of this review. There are some review articles on 2D vdW magnetic materials, which have involved the classification of materials and essential physical properties,[11,52–56] the fabrication method,[57–61] the modulation of magnetism,[3,8,31,62] the detection technology,[9,46,63] and spin-related devices.[1,2,22,23,31,57,63–65] In this review, from the perspective of magnetic structures, we pay more attention to some specific 2D vdW magnetic materials based on critical issues in the application of 2D vdW magnetism. At first, we present the state-of-the-art vdW magnetic materials in experiments and briefly discuss the current synthesis methods. Secondly, considering the critical issues in 2D vdW magnetic materials, such as low Curie temperature (T_C) and the control of anisotropy and magnetization, we introduce some critical vdW ferromagnetic and antiferromagnetic compounds in terms of intrinsic magnetism. Thirdly, we outline the approaches to manipulating fundamental magnetism and some preliminary application of spintronics. Finally, we highlight the challenges and provide an outlook on future directions for the field of 2D vdW magnetic materials.

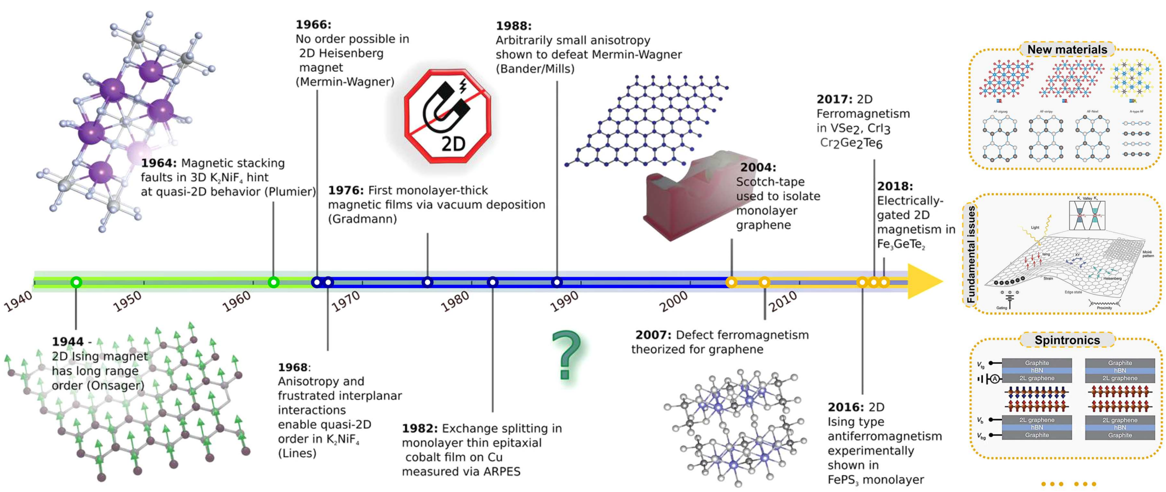

Fig. 1. The timeline of some important theoretical and experimental results in 2D magnetism began with Onsager's solution in 1944 and culminated with three main current research directions (reprinted with permission from Refs. [9,23,46,66]).

2. Magnetism and synthesis of vdW magnets

The family of vdW crystals has included a wide variety of materials over the past decade, but the vdW magnetic material is still in its infancy stage.[33,57,67] To date, vdW magnetic materials can be mainly categorized into metal chalcogenides and halides (including dihalides and trihalides), as displayed in Fig. 2.[9] The metallic elements mainly come from 3d transition metals such as Cr and Fe and gradually expanded to 4f rare-earth metals such as Ce and Dy recently.[20,44,52,68,69] The typical magnetism of pristine vdW magnets in experiments is also classified in Fig. 2. The spin model and magnetic configuration can be briefly described by a generalized Heisenberg spin Hamiltonian[8,60]

$$H = -\frac{1}{2}\sum\nolimits_{i,j}(J_{ij}S_iS_j + \Lambda_{ij}S_i^zS_j^z) - \sum\nolimits_i A_i\,(S_i^z)^2, \qquad (1)$$

where J_{ij} is the exchange constant between spins S_i (in the i^{th} lattice site) and S_j (in the j^{th} lattice site). Λ_{ij} and A_i are the anisotropic exchange and the single-ion anisotropies, respectively. Thus, the first term describes the exchange (Heisenberg) interactions, the second the anisotropic exchange, and the third the single-ion anisotropy. The additional asymmetric terms such as Kitaev[70] and Dzyaloshinskii–Moriya interactions[71] are also allowed. For the isotropic Heisenberg model with spatial dimension $n = 3$, magnetic anisotropy should be weak with Λ and $A \approx 0$. The XY ($n = 2$) model has strong easy-plane anisotropy ($A \rightarrow -\infty$), while the Ising ($n = 1$) model shows strong easy-axis anisotropy ($A \rightarrow +\infty$). These models provide a solid foundation for further investigating intrinsically 2D vdW magnetic materials. For $J > 0$, the spins favor parallel alignments, i.e., FM, whereas they favor antiparallel alignments (i.e., AFM) for $J < 0$. The vdW ferromagnets (FMs) have been found in chalcogenides and trihalides, and they are mainly Fe-based,[31,72–75] Cr-based,[20,21,76–78] and V-based.[79–83] Most 2D vdW FMs have very low T_C, such as CrI_3 (Ising-type, $T_C = 45$ K for monolayer CrI_3),[20] $CrBr_3$ (Heisenberg -type, $T_C = 27$ K for monolayer $CrBr_3$),[78] $Cr_2Ge_2Te_6$ (Heisenberg-type, $T_C = 30$ K for bilayer $Cr_2Ge_2Te_6$).[21] In contrast, itinerant ferromagnetic system Fe_xGeTe_2 ($x = 3$ and 5, Ising-type; $x = 4$) has received intensive interest because of its high T_C (near room temperature), high conductivity, and large magnetization.[31,72,73] Due to the macroscopic net magnetic moment, it is feasible to achieve the spin-related application of FM-based devices. Despite the difficulty in using antiferromagnets (AFMs) due to their vanishing net magnetization, AFMs hold promise for high-speed, low-power spintronics because they are robust against the magnetic field perturbation, absence of parasitic stray fields, and have higher magnetic resonance frequencies (THz regime) than that of the FMs (GHz regime).[2] Furthermore, the AFMs are much more abundant than the FMs in the vdW magnetic family. They belong to two kinds of magnetic structures, one is intralayer FM order with interlayer AFM order (i.e., A-type AFM), and the other is intralayer AFM order with C-type and G-type AFM. In a C-type structure, the interlayer coupling is FM, but in a G-type the interlayer coupling is AFM. For honeycomb crystal lattices, intralayer AFM order can be further divided into Néel, zigzag and stripy states.[3] The few-layer CrI_3 favors A-type AFM,[84] different from its FM in bulk related to the stacking state.[56] As the layered topological insulators,[85,86] $MnBi_2Te_4$ (Heisenberg-type),[87–90] $MnBi_4Te_7$[91,92] and $MnBi_6Te_{10}$[91,93] are intrinsic A-type AFM as well.[94,95] Interestingly, MPS$_x$ (M = transition metal, $x = 3$, 4) compounds contain rich antiferromagnetic states, such as A-type $CrPS_4$,[96,97] C-type zigzag (Co/Ni)PS_3 (XY-type),[98–100] C-type Néel $MnPS_3$ (Heisenberg-type),[101–104] and G-type zigzag $FePS_3$ (Ising-type).[43,44] Except for the FM/AFM order and disordered spin-liquid-like phases, there are non-collinear magnetic structures. These include the helimagnets such as FeOCl[105] and $FeCl_3$,[106] magnetoelectric Fe(Cl/Br)$_2$,[107] multiferroic (Mn/Co/Ni)I_2[108–110] and in-plane frustrated AFMs VCl_2 and VBr_2.[111,112] Rare-earth halide CeSiI is a recently discovered vdW magnetic compound hosting a coexistence of itinerant electron and frustrated magnetism.[68] There is still plenty of materials to be explored in experiments, some of which have been predicted, such as Dirac half-metal CrSeTe,[113,114] valleytronic semiconductor $LaBr_2$.[115,116]

The common synthesis methods for 2D vdW magnetic compounds are summarized in Fig. 2. These methods can be classified into two types, the top-down and the bottom-up. The former grows bulk single crystal and then exfoliates it to obtain atomically thin layers. The single-crystal growth strategies of vdW magnets include the chemical vapor transport, flux method, solid-state synthesis, Bridgman method, etc. The first two are the most commonly used. The chemical vapor transport is an efficient way to grow most bulk crystals such as CrX_3 (X = Cl/Br/I),[117] Fe_xGeTe_2 ($x = 3$, 4, 5),[72,73,118–121] MPS$_3$ (M = Fe, Co, Ni),[43,99,122] MOCl (M = Cr, Fe),[123,124] and metal-intercalated (Nb/Ta/Ti)S_2.[125–127] The transport agents I_2, Br_2, and $TeCl_4$ usually transport elementary substances between the furnace's hot and cold ends.[128] Additional temperature-oscillation[124] and reverse transport[129,130] can promote growing good-quality centimeter-scale single crystals. The flux method is liquid-growth to obtain large and high-quality crystals.[60] When certain substances that are one (or two) of the constituents of target products are selected as excess flux, this method is further called the "self"-flux method.[59] The self-flux method avoids the introduction of exotic elements and usually is prioritized for growing vdW magnetic materials such as $Cr_2Ge_2Te_6$ with an atomic ratio of 2 : 6 : 36 for Cr : Ge : Te,[131,132] Fe_3GeTe_2 (F3GT) with an atomic ratio of 1 : 2 : 4 for Fe : Ge : Te,[133] and $MnBi_2Te_4$ with an atomic ratio of 1 : 10 : 16 for Mn : Bi : Te.[90] The exfoliation technique is key to obtaining monolayers or thin flakes. For most vdW magnetic materials, a high-quality atomically thin sample can be obtained by mechanical exfoliation because of the low dissociation energy associated with the vdW layered structure. The electrochemical method can be used to exfoliate vdW magnets with high dissociation energy,

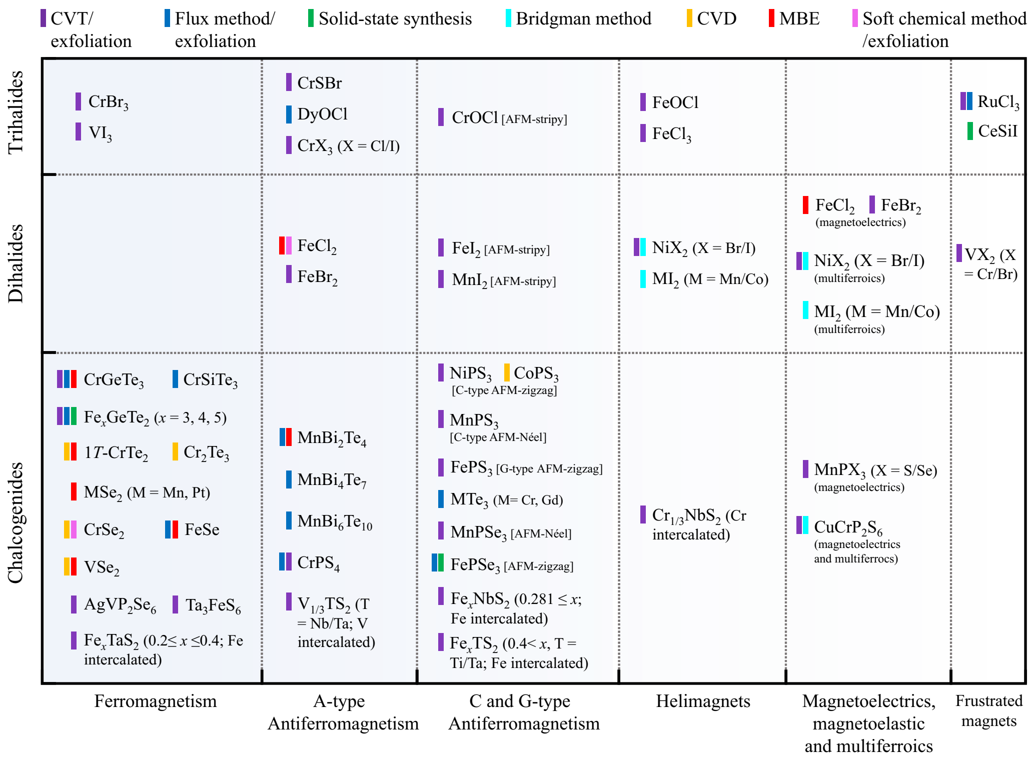

Fig. 2. Summary of pristine vdW magnets and their synthetic technique.

such as VSe_2.[134] Meanwhile, the electrochemical method can also introduce guest atoms into vdW layers to optimize the material properties. Wang *et al.*[135] synthesized (TBA)$Cr_2Ge_2Te_6$ compound by the interaction of tetrabutylammonium, and the T_C of (TBA)$Cr_2Ge_2Te_6$ is significantly increased from 67 K in pristine $Cr_2Ge_2Te_6$ to 208 K in (TBA)$Cr_2Ge_2Te_6$. For some complex 2D vdW magnetic compounds, the bottom-up methods offer a practicable strategy to grow the few-layer structure directly, including the chemical vapor deposition and molecular-beam epitaxy method. Those methods are controllable growth via adjusting the growth parameters in the process, widely used in synthesizing 2D vdW magnetic materials such as $CrTe_2$[136,137] and VSe_2.[138,139] However, for various compounds, epitaxy-grown usually needs specific growth substrates. The *in situ* growth via the chemical vapor deposition or molecular beam epitaxy method is recommended for high-quality heterostructure because transfer processes may introduce contamination by the exfoliation method.

3. The vdW ferromagnetic materials

The vdW FMs have been in the mainstream of modern magnetic research, especially due to their great vitality in spintronics. $Cr_2Ge_2Te_6$ is the first 2D ferromagnet to be discovered[21] and some intriguing phenomena have been found, such as the anomalous Hall effect in the $Cr_2Ge_2Te_6$ (< 50 nm)/Pt (5 nm) heterostructures,[140] the proximity effect in the $Cr_2Ge_2Te_6$ (30 nm)/graphene heterostructures.[141] Besides, some progress on devices has also been made toward magnetic manipulation, including current-induced magnetization switching in the $Cr_2Ge_2Te_6$ (< 50 nm)/Ta (5 nm) heterostructures,[142] $Cr_2Ge_2Te_6$ (12 nm)/$(Bi_{1-x}Sb_x)_2Te_3$ (6 nm) heterostructures,[143] and electric-field control of magnetism in the device based on few-layer $Cr_2Ge_2Te_6$.[144] However, low T_C (61 K in bulk $Cr_2Ge_2Te_6$ and 30 K in the bilayer $Cr_2Ge_2Te_6$) limits the practical applications of $Cr_2Ge_2Te_6$ in spintronic,[21,77] which is common in most of the vdW FMs. By constructing the $Cr_2Ge_2Te_6$ (< 7 nm)/NiO (50 nm) heterostructure, the T_C of the system can be improved to 115 K.[145] The 2D vdW chalcogenides MSe_2 (M = Mn, V),[83,146] $1T$-$CrTe_2$[136,137,147] and Fe_xGeTe_2 (x = 3, 4, 5)[31,72,73,148] are known as near room-temperature FMs. Among them, the monolayer $1T$-VSe_2 was synthesized and its magnetic hysteresis loops at 300 K were observed by Bonilla *et al.*[83] Because monolayer $1T$-VSe_2 was synthesized on HOPG and MoS_2 substrates using molecular-beam epitaxy, it cannot exclude the effect of interface strain to induce magnetism.[22] In fact, it is puzzling that the experimental magnetic moment is much larger than the calculated magnetic moment.[83,149–151] Some experiments based on x-ray magnetic circular dichroism did not detect long-range magnetism of $1T$-VSe_2 yet.[152,153] It was found that the charge density wave distortion can remove the intrinsic ferromagnetic ground state in $1T$-VSe_2.[154–156] Besides, the monolayer $1T$-VSe_2 was speculated as a frustrated magnet with its spins exhibiting subtle correlations.[154] Using an electrochemical exfoliation approach to obtain monolayer $1T$-VSe_2 flake, Yu *et al.*[134] revealed that a defectfree sample is significant to qualify the intrinsic magnetism of 1T-VSe_2. The origin of FM in 1T-VSe_2 requires further investigation. Also, a recent study observed ferromagnetic signatures in multilayer 2H-VSe_2 films.[157] On the contrary, 2H-$CrTe_2$ is a paramagnet as a result of the fully occupied d_{z^2} orbital of tetravalent Cr.[147] The bulk 1T-$CrTe_2$ is ferromagnetic with T_C of 310 K.[158] Using the mechanical exfoliation, fifteen-layer 1T-$CrTe_2$ retains the T_C of 305 K[159] and 170 nm 1T-$CrTe_2$ flake shows large anomalous Hall conductivity.[160] By molecular-beam epitaxy, monolayer 1T-$CrTe_2$ shows the T_C of 200 K[147] and the noncollinear spin reorientation under magnetic fields.[137] The 1T-$CrTe_2$/Bi_2Te_3 heterostructure by molecular-beam epitaxy possesses giant topological Hall effect signals.[161] The high T_C and conductivity Fe_xGeTe_2 ($x = 3$, 4, 5) system is attention-attracting in recent years. Especially in spintronics, Fe_xGeTe_2 family is regarded as a potential candidate to develop spin-related devices with a series of cutting-edge progress. Thus, we will introduce Fe_xGeTe_2 with $x = 3$, 4, 5 in detail, in terms of fundamental magnetism, modulation of magnetic properties and magnetism-related devices.

Fe_xGeTe_2 ($x = 3$, 4, 5) is a rare metallic example of itinerant vdW FMs with an intralayer three-dimensional network of the Fe sealed by a Te ligand sheet (Fig. 3(a)),[73,162] which enables high T_C of nearly room temperature (Fig. 3(b)).[73,148] Such itinerant magnetism is strongly coupled to the electronic structure and atomic-scale disorder and is affected by the site substitution. F3GT belongs to a hexagonal crystal structure ($P6_3/mmc$, No. 194) with the substructures of Fe and Ge atoms sandwiched by Te layers and the vdW gap between adjacent Te layers (Fig. 3(a)).[162] The Fe atoms occupy 2c and 4e inequivalent sites, marked Fe I and Fe II, respectively. In contrast to the complete occupation of Fe II, Fe I is partially filled in d-orbitals which dominates the FM.[22] By intercalating more Fe in-between the Te outer slab layers, Fe_4GeTe_2 (F4GT) and Fe_5GeTe_2 (F5GT) have been successfully synthesized.[73,163] F4GT has a rhombohedral structure ($R\bar{3}m$, No. 166) with lower symmetry than that of F3GT. F5GT remains the rhombohedral structure except that additional Fe III atoms are inserted above and below the Ge atom, leading to the splitting of Ge sites.[164] Except for rhombohedral symmetry, the space group $P3m1$ (No. 156) for F5GT was speculated,[165] but it has not been found in experiments so far. The high T_C is a significant feature of the Fe-rich Fe_xGeTe_2 system (Fig. 3(b)): For F3GT, the T_C is 230 K and 130 K for bulk crystal and monolayer, respectively;[166] the bulk F4GT shows an FM transition at $T_C \approx 270$ K, which remains almost the same with lowering the thickness to seven layers;[73] F5GT exhibits the highest T_C of 310 K in bulk ($T_C = 229$ K in bilayer F5GT grown by molecular beam epitaxy) among the Fe_xGeTe_2 ($x = 3$, 4, 5) system.[167,168] An increased number of neighboring magnetic ions increases the density of itinerant carriers, enhancing the strength of the exchange coupling, and consequently the magnitude of T_C, as shown in the inset of Fig. 3(b). The magnetic anisotropy is the critical parameter that maintains magnetic ordering in vdW magnetic materials. Tan *et al.*[120] reported a hard magnetic property with a near square-shaped magnetic hysteresis loop and large coercivity (up to 550 mT at 2 K) when the thickness of F3GT is reduced to less than 200 nm, revealing strong perpendicular anisotropy (PMA), consistent with the result of strong PMA in the ultrathin F3GT by Fei *et al.*[166] The bulk F5GT does not exhibit a PMA, unlike F3GT, and the PMA appears in the thin films.[169] Due to the spin reorientation, the magnetic anisotropy of F4GT is unique. It can be seen in Fig. 3(c) that F4GT bulk shows a spin reorientation transition at $T_{SR} = 110$ K with the easy magnetization axis rotated from *ab*-plane (FM1) to *c*-axis (FM2), related to the competition between the magnetocrystalline anisotropy and the shape anisotropy.[73] By reducing the thickness of F4GT, the T_{SR} is enhanced up to about 270 K and is consistent with a strong enhancement of PMA,[73] suggesting that the magnetic anisotropy of F4GT nanoflakes can be controlled with proper surface modification while remaining high T_C. Fe–Ge–Te family also has unique topological property. F3GT shows a large anomalous Hall current due to large Berry curvature induced by topological nodal lines.[170] You *et al.*[171] attributed the unexpected topological Hall effect in the configuration of large tilted magnetic fields in F3GT to either the possible topological domain structure of uniaxial F3GT or the noncoplanar spin structure forming during the in-plane magnetization. Recently, Bloch-type skyrmions have been observed in the *ab* plane of single-crystal F3GT[172,173] and F5GT (see Fig. 3(d)).[173] When the thicknesses of F3GT and F5GT samples are reduced to 21 nm and 61 nm, respectively, the Néel-type skyrmions emerge due to the interfacial Dzyaloshinskii–Moriya interaction (see Fig. 3(e)).[121,172] For F3GT, such Néel-type skyrmions can be driven by current pulses[174] and stabilized in WTe_2 (2.2 nm)/F3GT (24 nm)[175] and F3GT (70 nm)/$[Co/Pd]_{10}$ (16 nm)[176] heterostructures. The tunability of magnetic skyrmions shows great potential in developing high-density magnetic storage devices.

As Stoner-type itinerant FMs, the magnetic properties Fe_xGeTe_2 ($x = 3$, 4, 5) compounds are highly tunable utilizing external control parameters. As a well-known work, Deng *et al.*[177] found that the T_C of trilayer F3GT could be improved to room temperature from near 100 K by Li^+ ionic-liquid gating technology with a gate voltage of 1.75 V (Fig. 3(f)). Besides, the T_C of F3GT can also be well tailored by the micro-scale patterning[119] and strain.[178] Exerting a uniaxial tensile strain on F3GT thin flakes (about 50 nm), as shown in Fig. 3(g), increases the coercive field by more than 150% with an applied strain of 0.32% besides T_C.[178] On the contrary, a tiny current can reduce the coercive field in nanometer-thin F3GT[179] and the homojunction based on two few-layer F3GT flakes.[180] Figure 3(h) shows that the T_C of bulk F3GT decreases as a function of pressure, which is related to the lattice-shrinkage-induced variance of spin–lattice coupling.[181] Ding *et al.*[182] further found that the Fe–Ge(Te)–Fe bond angles deviated away from 90° under hydrostatic pressures, indicating the modification of the exchange interactions (the lower right in Fig. 3(h)). They proposed that the direct-exchange interaction became stronger at a higher pressure, leading to increased antiferromagnetic components and thus decreased T_C. As the exchange bias can realize in a single material $(MnBi_2Te_4)(Bi_2Te_3)_n$ ($n = 1$, 2),[183] Zheng *et al.*[184] displayed an exchange-bias behavior in vdW magnet F3GT nanoflakes by a protonic gate with the voltages $V_g = 4.3$ V, which demonstrates that a strong interlayer coupling can be realized by proton intercalation (Fig. 3(i)). Besides, the main pathway to achieve exchange-bias behaviors is constructing FM/AFM heterostructures which have been realized in lots of F3GT-based heterostructures, including $FePS_3$/F3GT,[185] MnP(S/Se)$_3$/F3GT,[186,187] CrOCl/F3GT,[188] and $CrCl_3$/F3GT.[189] The exchange-bias system has great potential in devices for low power consumption and ultrafast operation. Due to the Fe vacancies in Fe_xGeTe_2 compounds, intermetallic-like Fe–Ge slabs are amenable to chemical substitutions.[56] It is feasible to obtain Fe_xGeTe_2 with higher iron contents ($x > 5$) due to the existence of Fe vacancies in F5GT. In addition to controlling Fe content, Co and Ni substitution for Fe has aroused much interest due to similar Pauling's electronegativity and ionic radius. For F3GT, Co doping decreases the saturated magnetization and the T_C, but enhances the domain wall pinning effect. Therefore, the Co doping induces a hard magnetic phase, in stark contrast to the soft magnetic phase in bulk F3GT.[190] Similarly, both the ordered magnetic moment and the T_C are strongly suppressed in Ni-substituted F3GT (Fig. 3(j)). In particular, Drachuck *et al.*[191] performed the muon spin relaxation measurements and found that the FM order was continuously smeared into an FM cluster-glass phase beyond $x = 0.3$ in $(Fe_{1-x}Ni_x)_3GeTe_2$. The change in the magnetic order mentioned above is attributed to the intrinsically disordered structure of F3GT and subsequent dilution effects. For F4GT, with cobalt substitution reaching up to near 26%, the AFM is induced and the saturation magnetization is decreased (Fig. 3(k)).[165] The T_N of $(Fe_{0.61}Co_{0.39})_4GeTe_2$ is reduced slightly to ~ 210 K from the bulk value of 226 K with the thickness reduced down to nine layers. For F5GT, the cobalt doping at up to 30% for Fe enhances T_C and changes the anisotropy from the easy axis [001] to the easy *ab* plane, which may be related to Co substituting primarily on the Fe I sublattice.[192] In addition, the cobalt concentration of near 50% in $(Fe_{1-x}Co_x)_5GeTe_2$ also induces an antiferromagnetic ground state, which is originated from the combination of the primitive layer stacking and the high cobalt content.[192,193] In $(Fe_{1-x}Ni_x)_5GeTe_2$, the T_C and H_c increase firstly and then decreases with the Ni substitution for Fe, and a highest T_C of 478 K is obtained at $x = 0.36$. Chen *et al.*[194] attributed

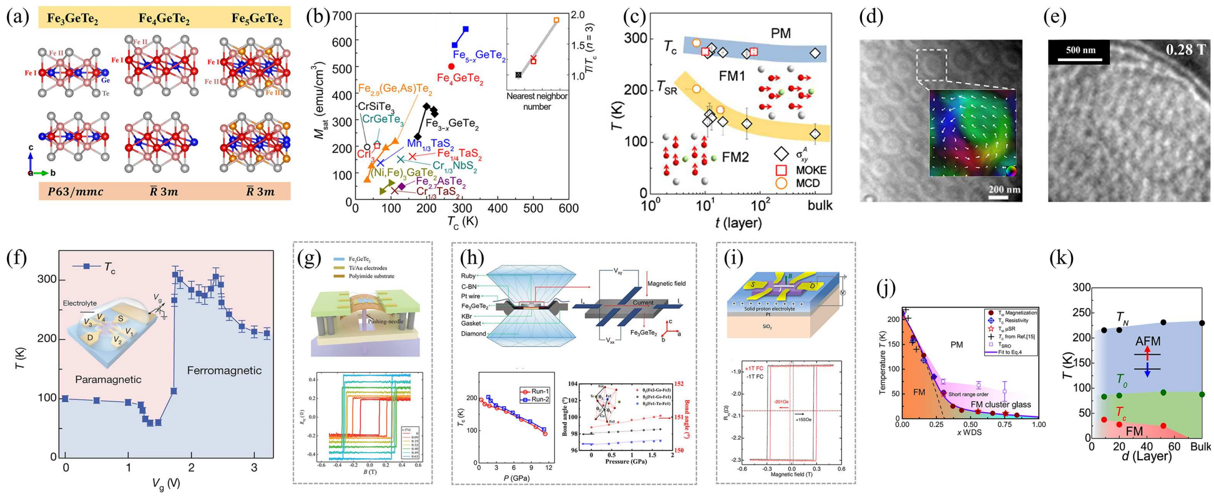

Fig. 3. (a) Three crystal structures in Fe_xGeTe_2 for $x = 3$, 4, and 5, respectively. (b) The T_C and saturation magnetization M_{sat} for various vdW FMs (reprinted with permission from Ref. [73]). (c) Thickness-temperature magnetic phase diagram of F4GT crystal (reprinted with permission from Ref. [73]). (d) The Bloch-type skyrmion bubbles of single-crystal F3GT at 93 K with zero-field. The inset is an enlarged in-plane magnetization distribution map processed by TIE analysis (reprinted with permission from Ref. [173]). (e) Generation of Néel-type skyrmions of F5GT flake thickness about 61 nm (0.28 T at 130 K) (reprinted with permission from Ref. [121]). (f) Phase diagram of the trilayer F3GT sample as the gate voltage and temperature is varied. The inset is the schematic of the F3GT device structure and measurement set-up (reprinted with permission from Ref. [177]). (g) Schematic diagram of F3GT device in the strain experimental set-up (the top) and Hall resistance R_{xy} versus external magnetic field B curves in the strain regime from 0% to 0.63% at 1.5 K (the bottom) (reprinted with permission from Ref. [178]). (h) Schematic of a high-pressure diamond anvil cell electrical properties measurement system for F3GT (the top) (reprinted with permission from Ref. [181]). The bottom is the T_C (reprinted with permission from Ref. [181]) and the Fe–Fe bond angle (reprinted with permission from Ref. [182]) of F3GT as a function of pressure in the experiment and theory, respectively. (i) Schematic of the Hall-bar device of F3GT nanoflakes on solid proton conductor used for Hall resistance measurements (the top), and the derived exchange-bias effect after ± 1 T field cooling (the bottom) (reprinted with permission from Ref. [184]). (j) Phase diagram of $(Fe_{1-x}Ni_x)_3GeTe_2$ determined from magnetization and transverse-field muon spin relaxation measurements and resistivity measurements (reprinted with permission from Ref. [191]). (k) The thickness-dependent magnetic phase diagram of the $(Fe_{0.61}Co_{0.39})_4GeTe_2$ crystal with characteristic temperatures of T_N, T_0 (i.e., T_{SR}), and T_C (reprinted with permission from Ref. [165]).

these to structural transition and the modulation of magnetic exchange couplings, which is different from the early results.[164] Thus, the element doping in F5GT is complex because of the strong structure disorder, which should be similar to F4GT with the same rhombohedral structure though there is little research on F4GT now. Hence, various intrinsic defects of Fe_xGeTe_2 ($x = 3, 4, 5$) system provide a natural platform to probe the underlying physics and further tuning magnetic properties of 2D vdW magnetic materials.

Spintronic devices based on giant magnetoresistance (GMR) and tunneling magnetoresistance (TMR) have been widely used in the magnetic hard drive and magnetic random-access memory, which are expected to be more efficiently integrated with 2D vdW magnetic materials to satisfy the demand of the big data era. A typical GMR structure consists of two FM layers separated by a non-magnetic metallic layer (TMR structure uses the insulating layer to replace the metal).[195] It exhibits two resistance states with respect to an external field, depending on the relative spin orientations in the FM layers. Due to high magnetization and conductivity, Fe_xGeTe_2 ($x = 3, 4, 5$) materials are suitable for constructing vdW heterostructures, enabling high-performance devices. Figure 4(a) shows the schematic of the F3GT/hBN/F3GT spin-valve consisting of an atomically thin hBN layer acting as a tunnel barrier and two exfoliated F3GT crystals acting as ferromagnetic electrodes.[196] In the F3GT/hBN/F3GT vdW heterostructure, typical behavior of the tunneling magnetoresistance can be observed at a magnetic field of ± 0.7 T. Its TMR can reach up to 160% at 4.2 K (Fig. 4(b)), larger than that of F3GT/InSe/F3GT (41% at 10 K),[197] F3GT/MoS_2/F3GT (3.1% at 10 K),[198] and F3GT/WS_2/F3GT (0.45% at 10 K).[199] Multiferroic tunnel junctions composed of FM electrodes and ferroelectric spacer, utilize both the TMR effect and tunneling electroresistance effect and can realize multi-level storage. However, the current progress of multiferroic tunnel junctions remained at the theoretical level and was discovered in various structures such as the $PtTe_2/Fe_xGeTe_2/In_2Se_3/Fe_yGeTe_2/PtTe_2$ (x, $y = 3, 4, 5$; $x \neq y$) heterojunction with four resistance states and an ultra-low resistance-area product.[200] It is worth investigating experimentally in the future. In particular, the spin-valve effect can also be achieved in the F3GT/F3GT/F3GT vdW homo-junctions as shown in Fig. 4(c),[201] because the width of the vdW interface in the homo-junctions is slightly larger than that of the vdW nature gaps in the F3GT, resulting in the independent magnetization switching of the individual F3GT nanoflakes. Figure 4(d) shows that the homo-junctions have three-state resistance, with the GMR of the two steps being 0.52% and 1.35%, respectively.[201] Besides, the F3GT/graphite/F3GT heterostructure displays a hitherto rarely seen antisymmetric MR effect with distinct high-, intermediate-, and low-resistance states.[202] Figure 4(e) shows the optical and atomic force microscopy images of a trilayer heterostructure with a Hall bar patterned on the top of the F3GT layer.[202] When the current flows in the graphite layer at the interfaces, the Rashba-split of 2D electron gas induced by the spin–orbit coupling causes spin momentum locking, leading to opposite spin orientations at the two interfaces and displaying an antisymmetric MR effect as shown in Fig. 4(f). Besides, because of the existence of exchange-bias behavior, antisymmetric magnetoresistance is also observed in the FM/AFM heterostructure.[186]

The spin–orbit torque (SOT) spawns a whole new branch of spintronics to achieve high-performance magnetic memories, which has been realized in F3GT materials. Wang *et al.*[203] devised a bilayer structure of F3GT (3.2–4.8 nm)/Pt (6 nm), as shown in Fig. 5(a). They found the current-induced magnetization switching of F3GT with the in-plane magnetic field of 50 mT at 100 K (Fig. 5(b)). The

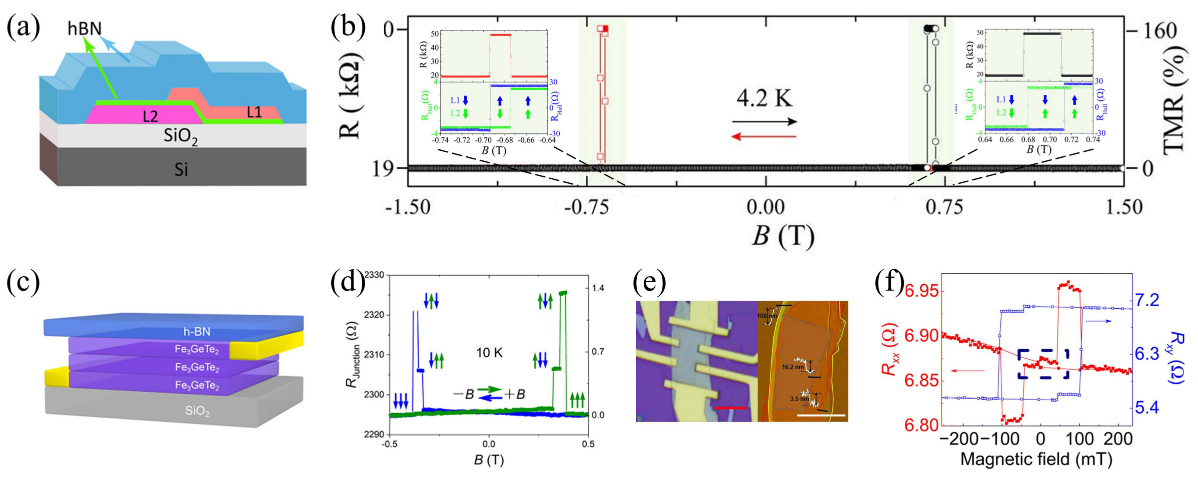

Fig. 4. (a) Schematic representation of the F3GT (7 nm)/hBN/F3GT (20 nm) heterostructures and (b) the spin-valve effect corresponding to tunneling resistance and Hall resistance at 4.2 K with an applied field perpendicular to the layers (reprinted with permission from Ref. [196]). (c) The F3GT/F3GT/F3GT three-state spin valves and (d) its resistance as a function of the perpendicular magnetic field measured at 10 K (reprinted with permission from Ref. [201]). (e) Overview of the MR effect in F3GT/graphite/F3GT heterostructures and (f) the field-dependent resistance R_{xx} and R_{xy} measurements of an F3GT/graphite/F3GT heterostructure at 50 K (reprinted with permission from Ref. [202]).

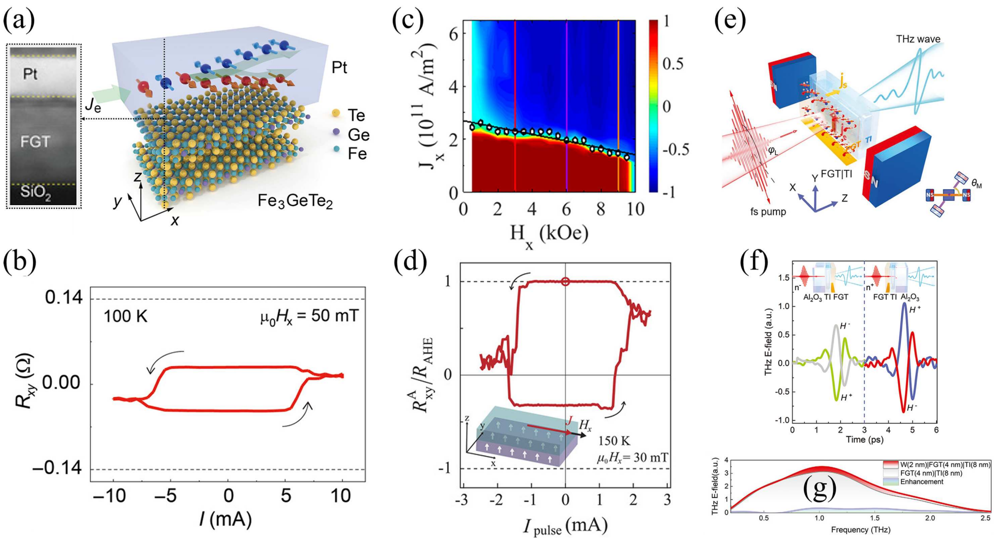

Fig. 5. (a) Schematic view of the F3GT/Pt bilayer structure with the cross-sectional dark-field scanning transmission electron microscopy image pointed by the black arrow (reprinted with permission from Ref. [203]). (b) Current-driven perpendicular magnetization switching in the F3GT/Pt bilayer device with the in-plane magnetic field of 50 mT (reprinted with permission from Ref. [203]). (c) Effective switching current as a function of applied in-plane positive bias field in the F3GT (15–23 nm)/Pt (5 nm) heterostructures (reprinted with permission from Ref. [204]). The color scale represents the switching resistance as a percentage of the absolute value of the anomalous Hall resistance at zero current. (d) The ratio of anti-symmetrized Hall resistance R_{xy}^{A} to the anomalous Hall resistance R_{AHE} measured in WTe_2/F3GT heterostructure with a sweeping current pulses I_{pulse} under in-plane magnetic field of 30 mT (reprinted with permission from Ref. [10]). (e) Schematic diagram of the femtosecond laser pulse excitation and THz radiation from the F3GT/Bi_2Te_3 heterostructure (reprinted with permission from Ref. [205]). (f) Radiated THz electric field signals with opposite magnetization when the pump pulse was incident on the FGT side or the substrate side (reprinted with permission from Ref. [205]). (g) The spectra of THz waveforms generated from W/F3GT/Bi_2Te_3, F3GT/Bi_2Te_3, and the enhanced differential signal, respectively (reprinted with permission from Ref. [205]).

switching originates from the current-induced SOT generated by the current flowing in the Pt layer. Similarly, Alghamdi *et al.*[204] also found the SOT in the F3GT (15–23 nm)/Pt (5 nm) heterostructures with $\sim 2.5\times10^{11}$ A/m^2 current density at 180 K (Fig. 5(c)). Recently, a much smaller switching current (3.90×10^{6} A/m^2 at 150 K) and power dissipation were achieved in a vdW heterostructure of the topological semimetal WTe_2 and ferromagnet F3GT (Fig. 5(d)), which indicates feasibility and efficiency of 2D vdW FMs/topological materials.[10] In addition, the heterostructures comprised of the F3GT films on topological insulator Bi_2Te_3 crystals can realize ultrafast THz spin dynamics. Figure 5(e) shows the scheme of F3GT/Bi_2Te_3 heterostructures and the experimental geometry of the THz emission spectroscopy.[205] Flipping the sample orientation can switch the polarity of THz spectroscopy, confirming that the generation of THz spin-current pulses originates from the spin-to-charge conversion induced by electric-dipole breaking the space-inversion symmetry (Fig. 5(f)). The W (2 nm)/F3GT (4 nm)/Bi_2Te_3 (8 nm) heterostructures were further fabricated to improve the THz spin-current injection (Fig. 5(g)). The integration of vdW-type topological materials and magnets offers a promising route to achieving energy-efficient and high-speed spintronic devices. Recently, Zhao *et al.*[206] designed a room-temperature lateral spin-valve device using F5GT/graphene heterostructures and achieved the tunnel spin polarization of about 45%, which enables electrical control of spin signal and realization of basic building blocks for F5GT device application. Since F4GT and F5GT are recently discovered, those spin-related applications are in the early stages and need more effort.

4. The vdW antiferromagnetic materials

Compared to the FMs, the AFMs have the following advantages: (1) The AFMs have zero net magnetic moments, so they are immune to external magnetic fields, and their stray field is negligibly weak, which are expected to realize high-density and stable antiferromagnetic memory devices. (2) They have a higher magnetic resonance characteristic frequency and can work at the THz frequency range. (3) Most AFMs are insulators, which can prevent the transport of charges, maintain the spin current transport, and reduce the Joule heat dissipation. Antiferromagnetic spintronics has been an emerging and rapidly developing field, which has become more encouraging with the introduction of 2D vdW AFMs. It is well known that the measurement and modulation of the physical properties of AFMs, such as the magnitude and direction of magnetic moments, are challenging experimentally due to the zero net magnetic moment. Neutron scattering technology is the only method that can directly observe antiferromagnetic and crystal structures simultaneously and enable quantitative studies. The study of the magnetic structures is helpful to understanding different exchange interactions in the compound and its various magnetic behaviors, thus guiding for further improving the material properties. In recent years, the research on 2D vdW magnetic materials has focused on optical and electrical detection methods, such as Raman spectroscopy, Hall resistance, magneto-optic Kerr effect, magnetic circular dichroism, etc.[31] The primary detection tool for thin layers of AFM is Raman spectroscopy, which is sensitive to spin-lattice coupling and spin-wave excitation.[207] When the magnetic phase transition breaks both space inversion and time-reversal symmetries, the second harmonic generation (SHG) spectroscopy can also serve as a powerful tool in detecting AFM.[3,32,208–210] Among vdW AFMs, those with A-type magnetic structures are of particular interest due to intralayer ferromagnetic exchange coupling with interlayer antiferromagnetic exchange coupling. The only antiferromagnetic exchange coupling in A-type AFMs is interlayer coupling mediated by the vdW gap, which makes it usually small especially compared to those with intralayer antiferromagnetic exchange coupling. Therefore, the saturated fields are generally small for A-type AFMs (0.3 T for $CrCl_3$,[211] 0.58 T for CrSBr,[212] 2 T for CrI_3,[213–215] 7.7 T for $MnBi_2Te_4$,[216] 8.5 T for $CrPS_4$[97]), which can provide some advantages for the manipulation of the magnetic properties. They may exhibit field-induced spin-flop or spin-flip transition for weak or strong magnetocrystalline anisotropy. When the magnetic field is along the easy axis, the critical field of spin-flop $H_{\rm flop}$ or saturated field $H_{\rm S}$ is given by[217]

$$H_{\rm flop} = \sqrt{2H_{\rm AF}H_{\rm A} - H_{\rm A}^2}, \tag{2}$$

$$H_{\rm S} = 2H_{\rm AF} - H_{\rm A}, \tag{3}$$

where $H_{\rm AF}$ and $H_{\rm A}$ are antiferromagnetic exchange field and magnetocrystalline anisotropy field, respectively. An increase in $H_{\rm A}$ increases $H_{\rm flop}$, while $H_{\rm S}$ is reduced. When $H_{\rm A} = H_{\rm AF}$, $H_{\rm flop} = H_{\rm S}$. With the further increase of $H_{\rm A}$, $H_{\rm S}$ will become smaller than $H_{\rm flop}$, resulting in a spin-flip transition with $H_{\rm flip} = H_{\rm S}$. The low-field-induced magnetic transitions in A-type AFMs make them intriguing. Besides, the ferromagnetic surface layer makes A-type AFMs suitable for realizing proximity effects and building vdW magnetic heterostructure. Based on their critical fields, we will introduce some specific A-type AFMs that are little focused, unlike CrI_3 and $MnBi_2Te_4$.

The $T_{\rm N}$ of bulk $CrCl_3$ is 17 K with easy-plane anisotropy (see Fig. 6(a)).[211,218] However, the magnetocrystalline anisotropy of $CrCl_3$ is weak, which is dominated by the shape anisotropy,[218] resulting in a negligible spin-flop transition around 100–200 Oe in the bulk $CrCl_3$.[211] Above $T_{\rm N}$, there is another short-range magnetic ordering of in-plane FM. Wang *et al.*[218] constructed the graphite/$CrCl_3$/graphite tunnel junctions. The odd–even layer effect of spin-flop transition was first observed in few-layer $CrCl_3$ by TMR due to a finite Zeeman energy contributed by the uncompensated magnetic moment in odd layer A-type antiferromagnet (Fig. 6(b)). Odd–even layer effects were observed later in $MnBi_2Te_4$[219] and $MnSb_2Te_4$.[220] Due to the simple magnetic structure, the magnetic behavior of A-type antiferromagnet can be well described by the "macro-spin" linear chain model.[218] The easy-plane anisotropy of $CrCl_3$ offers a good opportunity to examine 2D-*XY* FM. Monolayer $CrCl_3$ grown on graphene/6H-SiC(0001) shows ferromagnetic ordering with critical scaling characteristics of a 2D-*XY* system, indicating the realization of a finite-size Berezinskii–Kosterlitz–Thouless phase transition.[221] Recent calculations show that the magnetic anisotropy of $CrCl_3$ can be tuned to be out-of-plane by applying a compressive strain, further offering a versatile platform to study both 2D Ising and *XY* FM.[222] In $CrCl_3$/bilayer graphene heterostructures, as shown in Fig. 6(c), the large nonlocal signals can be observed in magneto-transport nonlocal measurement under perpendicular magnetic fields, which mainly originate from the exchange-field-induced Zeeman spin Hall effect (Fig. 6(d)).[223] Besides, the strong interfacial spin–orbit coupling in $CrCl_3/NbSe_2$ can lead to Fulde–Ferrell–Larkin–Ovchinnikov state.[224]

Although CrSBr is a relatively new material with detailed physical properties reported in 2020,[212] it has already become a rising star as an air-stable semiconductor. The $T_{\rm N}$ of single-crystal CrSBr is 132 K, and the magnetic ground state is A-type AFM with an easy *b*-axis which is confirmed by neutron diffraction.[225] The magnetocrystalline anisotropy of CrSBr is relatively strong with prominently anisotropic magnetic behavior along three crystallographic axes, resulting in a spin-flip transition with a magnetic field of around 0.35 T along the *b*-axis at 2 K.[212] Using the SHG, Lee *et al.*[226] found an intermediate magnetic phase (labeled iFM in Fig. 6(e)) in which individual layers are ferromagnetically ordered internally, but the interlayer coupling remains paramagnetic, which also exists in $CrCl_3$.[211,226] Interestingly, a hidden ferromagnetic order related to the ferromagnetic ordering of magnetic defects is found below 35 K related to carrier-mediated FM ordering of magnetic defects (Fig. 6(f)).[212] The electrostatic gate can tune such a hidden FM.[227] A recent study shows a crossover of spin dimensionality from 2 to 1 in CrSBr at 40 K, corresponding to a transition from *XY* to an Ising-type model.[225] The shape of exfoliated CrSBr flake is usually rectangular, showing the in-plane lattice anisotropy. Similarly, the electronic transport in CrSBr exhibits quasi-1D behavior, which can be considered systems formed by weakly and incoherently coupled 1D wires.[228] Figure 6(g) shows a strain device that can apply continuous, *in situ* uniaxial tensile strain to CrSBr.[229] The photoluminescence spectra shows a clear 12 meV redshift between the low- and high-strain states, indicating an antiferromagnetic-to-ferromagnetic phase transition which is ascribed to the strong effect of in-plane lattice constant on the interlayer magnetic exchange interaction.[229] Bilayer graphene is magnetized by the proximity of CrSBr, leading to the efficient electrical and thermal spin-current generation with a strong spin polarization up to 14% (Fig. 6(h)),[230] which shows the great potential of CrSBr in the 2D spintronics and spin-caloritronics.

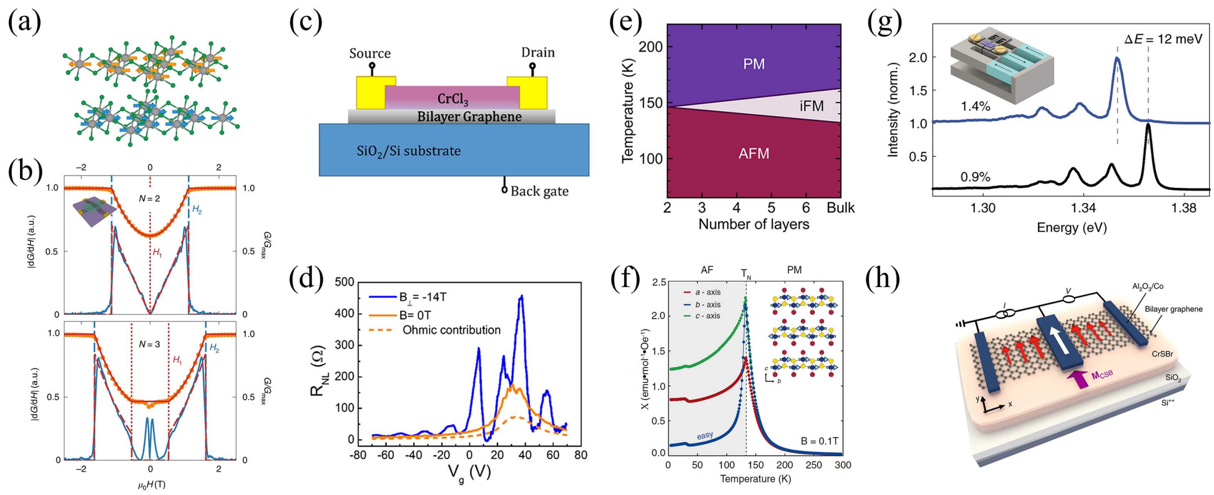

Fig. 6. (a) The crystal and magnetic structures of $CrCl_3$ (grey spheres represent the Cr atoms arranged in a honeycomb structure, while Cl atoms are represented in green) (reprinted with permission from Ref. [218]). (b) Measured (orange circles) and calculated (red solid line) magnetoconductance of graphite/$CrCl_3$/graphite tunneling junction with bi- (the top) and trilayer (the bottom) $CrCl_3$ (reprinted with permission from Ref. [218]). (c) Schematic diagram of $CrCl_3$/bilayer graphene heterostructure device and (d) its nonlocal resistance as a function of gate voltage at zero magnetic field and perpendicular magnetic field (reprinted with permission from Ref. [223]). (e) Magnetic phase diagram of CrSBr presented as a function of layer number and temperature (65–220 K) (reprinted with permission from Ref. [226]). (f) Magnetic susceptibility of single-crystal CrSBr versus temperature along the *a*-axis (solid red dots), *b*-axis (solid blue dots), and *c*-axis (solid green dots). The inset shows the magnetic structure of the Cr spins in the AFM state with the easy axis (*b*-axis) (reprinted with permission from Ref. [212]). (g) Photoluminescence spectra at 0.9% (black) and 1.4% strain (blue). The inset is the schematic of the strain cell based on three parallel piezo stacks glued to a titanium backing and flexure. The strain is applied to vdW materials placed on a gapped SiO_2/Si substrate fixed on top of the strain device (reprinted with permission from Ref. [229]). (h) Schematics of a three-terminal spin valve constructed by a bilayer graphene/bulk CrSBr heterostructure and ferromagnetic electrodes (Al_2O_3/Co) (reprinted with permission from Ref. [230]).

The layered metal dichalcogenides $CrPS_4$ is somehow overlooked for a long time. There are many arguments about the magnetic structure,[231–233] and it was not determined until 2020.[96,97] Based on neutron diffraction measurement, as shown in Fig. 7(a), the magnetic moments of $CrPS_4$ lie in the *ac* plane with a slight deviation of 9.5° from the *c* axis at 1.7 K (Fig. 7(b)).[97] The T_N of bulk $CrPS_4$ is 38 K, and the magnetocrystalline anisotropy of $CrPS_4$ is weak, which results in a small H_{flop} of 0.8 T at 2 K. Due to the in-plane anisotropy, spin-flop-induced moment realignment is parallel to the quasi-1D chains of CrS_6 octahedra on the *b*-axis (Fig. 7(b)).[96,234] In-plane anisotropic behaviors of optical properties in $CrPS_4$ have also been observed.[235–237] There is a hidden spin reorientation transition T_{SR} at around 35 K in $CrPS_4$ with magnetic moments realigning to the *b*-axis upon heating (Fig. 7(c)).[234,238] The spin reorientation transition is first-order and can be considered as a spontaneous spin-flop transition without a magnetic field due to the similar realignment of magnetic moments. The T_{SR} can be effectively suppressed by applying pressure while T_N decreases slightly.[234,238] Therefore, the easy *b*-axis magnetic phase of $CrPS_4$ can be stabilized by pressure, further offering another way to manipulate the Néel vector. Such temperature- and pressure-driven spin reorientation transition is rare in 2D vdW magnetic compounds, which could become more dramatic in the 2D limit. In monolayer $CrPS_4$, FM is well preserved and air-stable.[239] The exchange coupling constants of few-layer $CrPS_4$ seem to be the same as those of bulk.[239] However, the magnetic properties, such as the spin-flop transition of multilayer $CrPS_4$, still require further study. A possible route is using TMR, and magnetic tunnel junctions based on $CrPS_4$ are predicted to have large TMR (370000% in Au/$CrPS_4$(ten layers)/Au) with odd–even oscillation (Fig. 7(d)).[240] The magnetic proximity effect is also promising due to the in-plane FM order. The spin-flop transition of $CrPS_4$ flakes is observed in the magneto-transport of heavy metal Pt and Pd in $CrPS_4$/heavy metal heterostructures.[241] Notably, $CrPS_4$ can serve as an alternative for hBN in protecting and transferring 2D vdW materials, showing great potential in assembling vdW heterostructures.[242] Besides, $CrPS_4$ provides a large exchange field in $NbSe_2$/$CrPS_4$ heterostructure, leading to clear nonreciprocal transport.[243] Exchange-bias effect was also found in $CrPS_4$ flakes covered with 5 nm NiFe.[244]

Except for A-type AFMs mentioned above, MPS_3 ($M =$ transition metal) vdW family with C-type and G-type AFM is the most studied. The primary magnetic properties have been summarized in some reviews.[245,246] We will briefly introduce C-type antiferromagnetic $MnPS_3$ here, a good candidate for antiferromagnetic spintronics. $MnPS_3$ is predicted to hold the spin Nernst effect of magnons,[247] and later experiments on bulk $MnPS_3$ show evidence of the magnon Nernst effect.[248] Xing *et al.*[249] observed the long-distance magnon transport in $MnPS_3$ with the magnon relaxation length of 2.8 ± 0.4 μm at 2 K by nonlocal measurements.[249] Furthermore, the vdW magnon valve was realized using $MnPS_3$ (Fig. 7(e)), in which the second harmonic magnon signal can be turned off by DC gate current through a metal gate, as shown in Fig. 7(f).[250] Such a fully electrical switching of the magnon signal can promote complex manganic applications, especially the logic gates. Unlike $FePS_3$ and $NiPS_3$ with zigzag-type AFM, the magnetic ordering breaks both spatial-inversion and time-reversal symmetries in $MnPS_3$ with Néel-type AFM, making it possible to be probed by SHG.[209] With sensitive SHG microscopy, the antiferromagnetic domains can be further imaged (Fig. 7(g)).[251] Pronounced tunneling magnetoresistance in monolayer $MnPS_3$ indicates the magnetism is persisted in the monolayer limit,[104] which is also theoretically possible owing to the dipolar interactions in $MnPS_3$.[252,253] However, Raman[102] and SHG[251] indicate that the monolayer is non-magnetic. An anomalous mirror symmetry breaking in samples thinner than ten layers shows the disorder effect in few-layer $MnPS_3$ (Fig. 7(g)).[251] All these puzzles in the few-layer $MnPS_3$ need further studies.

The MOX (M = V, Cr, Fe, Dy; X = Cl, Br) is also a vdW antiferromagnetic family with relatively complex magnetic structures. Therefore, the relevant research is very little on the concept of 2D magnetism. They usually possess orthorhombic structures, while most magnets are monoclinic. Strong magnetoelastic coupling is observed in VOCl,[254] FeOCl,[255] and CrOCl.[256] CrOCl is a stripy antiferromagnet with T_N = 13.5 K, and the magnetic cell is a, $4b$, c.[257] At 27.7 K, there is another transition related to incommensurate magnetic superstructures.[256] A recent study shows that CrOCl is air-stable and has strong in-plane anisotropy.[258] Due to the field-induced magnetic phase transition, the magnetic state of few-layer CrOCl can be probed by TMR. Figure 7(h) is a magnetic phase diagram probed by TMR in four-layer CrOCl, which shows that a spin-flop transition will occur first, followed by a magnetic phase transition from $\uparrow\uparrow\downarrow\downarrow$ to $\uparrow\uparrow\uparrow\downarrow\downarrow$ magnetic state under a magnetic field along the c direction.[123] The drastic change of tunneling current in monolayer CrOCl indicates its magnetism can persist in the monolayer limit.[259] FeOCl has a complex spiral magnetic structure with a magnetic unit cell 28 times the size of the nuclear one.[105] A recent study shows that FeOCl possesses strong in-plane optical and electrical anisotropy.[124] It would be interesting to explore the interplay between noncolinear magnetic structure, anisotropy, and dimensionality in few-layer FeOCl. DyOCl is also an A-type antiferromagnet recently determined by neutron diffraction with the Néel temperature of 10 K. Due to the high atomic number of rare-earth Dy, DyOCl exhibits strong magnetocrystalline anisotropy with magnetic moment of 9.2 μ_B for the b-axis field but only 0.2 μ_B for the c-axis field of 50 kOe at 2 K.[69] The magnetization undergoes two transitions whereas the first one exhibits hysteresis, which is more complex than the simple spin-flip transition and needs further investigation.

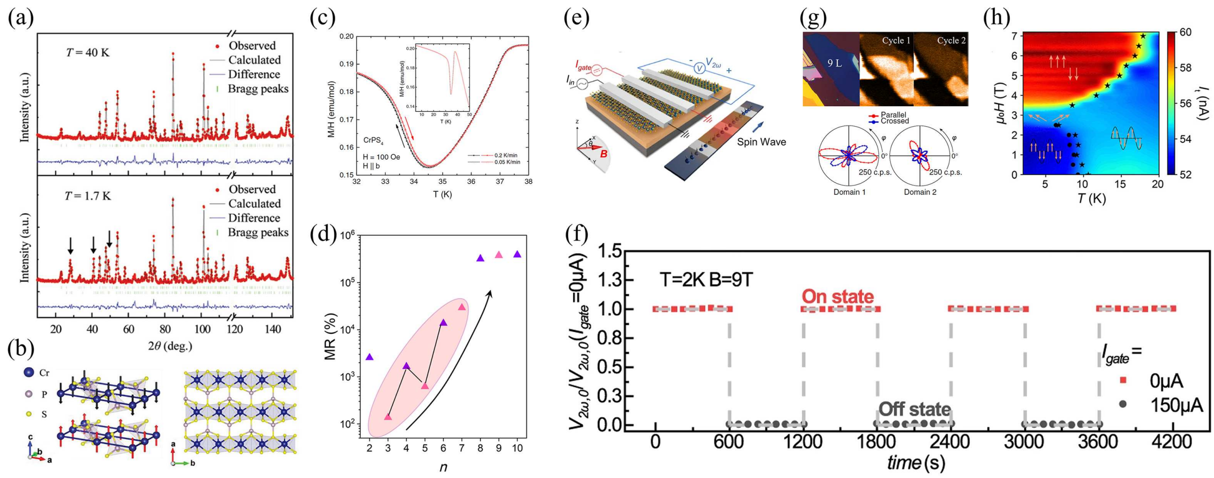

Fig. 7. (a) Neutron diffraction patterns of $CrPS_4$ powder sample at 40 K and 1.7 K, respectively. The black arrows represent magnetic diffraction peaks due to antiferromagnetic ordering (reprinted with permission from Ref. [97]). (b) Crystal and magnetic structure of $CrPS_4$ (the left) and the ab plane of $CrPS_4$ monolayer (the right) (reprinted with permission from Ref. [97]). (c) Temperature-dependent susceptibility of CPS_4 single crystal, measured at external field H = 100 Oe with $H//b$ on cooling and warming in the vicinity of the magnetic transitions (reprinted with permission from Ref. [238]). (d) The TMR in a log scale as a function of the $CrPS_4$ layer number n in Au/n-layer $CrPS_4$/Au) magnetic tunnel junction (reprinted with permission from Ref. [240]). (e) Artistic schematics of the thermal magnon generation, manipulation, and detection in $MnPS_3$. The upper left section shows the device structure with external circuits and the direction of the external in-plane magnetic field; the lower right section shows the propagation and modification of spin waves by the gate (reprinted with permission from Ref. [250]). (f) Operation of the $MnPS_3$ magnon valve with the DC gate current I_{gate} repeatedly toggles between 0 μA (on state) and 150 μA (off state) (reprinted with permission from Ref. [250]). (g) The top is the optical image of the nine-layer $MnPS_3$ sample (scale bar: 20 μm) and its SHG intensity mapping measured at 5 K (reprinted with permission from Ref. [251]). The bottom is the SHG polar patterns of antiferromagnetic $MnPS_3$ domains in nine layers measured at 5 K (reprinted with permission from Ref. [251]). (h) Magnetic phase diagram of four-layer CrOCl probed by TMR (reprinted with permission from Ref. [123]).

5. Summary and outlook

Exploration and investigation into intrinsic FM and AFM of the 2D vdW materials are of utmost importance for understanding low-dimensional magnetism and developing next-generation spintronic devices at the atomic scale. This review focused on magnetism in vdW magnetic materials and summarized fundamental magnetism, the modulation of magnetism, and the spin-related device. Although there has been impressive progress in emancipating several concepts and understanding in the field of 2D vdW magnetic materials, many scientific and technical challenges in the aforementioned research directions for 2D vdW magnetic materials still need researchers to spare no effort.

Exploration of new vdW magnetic materials Until now, the 2D vdW magnetic materials as a striking member of the 2D vdW family are rare. Thus, it is necessary to enrich the family. For most reported vdW magnetic materials, instability and low magnetic ordering temperatures have been central obstacles in deep research and the potential application of 2D magnetism. It is essential to address those issues by discovering more 2D vdW magnetic members. The investigation of the existing system is also significant to deal with the above problem, such as in itinerant ferromagnetic systems with high T_C.

Fundamental issues of condensed matter physics From the perspective of magnetic states, there are 1651 magnetic space groups to describe bulk magnetic structures and 528 magnetic layer groups to describe 2D magnetic structures, far more extensive than space groups.[11] Therefore, the exploration of in-depth intrinsic magnetism is very complicated but essential. However, most detection methods can only offer qualitative results on the few-layer magnetism of vdW magnetic materials.[63] Thus, quantitative characterization with nanometer spatial resolution is still in demand and is expected to acquire an in-depth understanding of 2D magnetism. Moreover, there are few techniques to measure the magnetic properties of AFMs directly. Thus, some novel and sophisticated techniques for *in situ* detection, like quantum magnetic imaging technique based on nitrogen-vacancy center,[260,261] need to be developed.

The combination of 2D vdW magnetic materials and other functional materials is a significant issue. Controllable stacking of materials with different properties such as magnetic ordering, charge ordering, superconductivity, spin-valley coupling, and topological band structure is encouraged because it can help us understand in-depth physical phenomena accompanied by many particular properties such as new spin textures and exotic Berry phases.

The cutting-edge application of 2D vdW magnets The combination of FMs and AFMs can induce the exchange-bias effect, which is promising for future applications in high-density storage. Similar to superconductivity in twisted bilayers of graphene,[262] it is possible to manipulate and understand the coupling of FM and AFM in the 2D limit by twisting engineering to combine and extend the properties of their constituent parts, which has a little preliminary progress on twisted bilayer FM/FM CrI_3[261,263] or double bilayer AFM/AFM CrI_3.[264] Moreover, the interplay between magnetism and topology in twisted heterostructures deserves attention. For example, the magnetic skyrmions are topological spin textures, which are likely to be observed by twisting two magnetic layers.[265,266] Combined with the external electric field, strain, and pressure, the above properties can be further modulated. In particular, the unique magnetic structures of AFMs will play a vital role in the future. A predictable assumption is switching the spins in upper and lower layers in the A-type antiferromagnetic structure by applying the SOT effect separately,[3] which is further expected to be applied to the THz regime.

We envision that 2D vdW magnets would help to promote a revolutionary development for the highly integrated electronic and spintronic devices in information computation, communication, and storage technologies.

Acknowledgements

The authors acknowledge the funding support of the National Natural Science Foundation of China (Grant Nos. 11975035, 51731001, 11805006, and 11675006) the National Key Research and Development Program of China (Grant Nos. 2017YFA0206303 and 2017YFA0403701).

References

[1] Li H, Ruan S and Zeng Y J 2019 *Adv. Mater.* **31** 1900065
[2] Gong C and Zhang X 2019 *Science* **363** 706
[3] Rahman S, Torres J F, Khan A R and Lu Y 2021 *ACS Nano* **15** 17175
[4] Goodenough K M, Wall F and Merriman D 2017 *Nat. Resour. Res.* **27** 201
[5] Lewis L H and Jiménez-Villacorta F 2012 *Metall. Mater. Trans. A* **44** 2
[6] Gutfleisch O, Willard M A, Bruck E, Chen C H, Sankar S G and Liu J P 2011 *Adv. Mater.* **23** 821
[7] Patel K, Zhang J and Ren S 2018 *Nanoscale* **10** 11701
[8] Gibertini M, Koperski M, Morpurgo A F and Novoselov K S 2019 *Nat. Nanotechnol.* **14** 408
[9] Mak K F, Shan J and Ralph D C 2019 *Nat. Rev. Phys.* **1** 646
[10] Shin I, Cho W J, An E S, Park S, Jeong H W, Jang S, Baek W J, Park S Y, Yang D H, Seo J H, Kim G Y, Ali M N, Choi S Y, Lee H W, Kim J S, Kim S D and Lee G H 2022 *Adv. Mater.* **34** 2101730
[11] Wang M C, Huang C C, Cheung C H, Chen C Y, Tan S G, Huang T W, Zhao Y, Zhao Y, Wu G, Feng Y P, Wu H C and Chang C R 2020 *Ann. Phys.-Berlin* **532** 1900452
[12] Mak K F, Lee C, Hone J, Shan J and Heinz T F 2010 *Phys. Rev. Lett.* **105** 136805
[13] Zhang Y, Tang T T, Girit C, Hao Z, Martin M C, Zettl A, Crommie M F, Shen Y R and Wang F 2009 *Nature* **459** 820
[14] Song C, Xiao W, Li L, Lu Y, Jiang P, Li C, Chen A and Zhong Z 2019 *Phys. Rev. B* **99** 214435
[15] Bolotin K I, Sikes K J, Jiang Z, Klima M, Fudenberg G, Hone J, Kim P and Stormer H L 2008 *Solid State Commun.* **146** 351
[16] Jones A M, Yu H, Ghimire N J, Wu S, Aivazian G, Ross J S, Zhao B, Yan J, Mandrus D G, Xiao D, Yao W and Xu X 2013 *Nat. Nanotechnol.* **8** 634
[17] Yang S, Hu C, Wu M, Shen W, Tongay S, Wu K, Wei B, Sun Z, Jiang C, Huang L and Wang Z 2018 *ACS Nano* **12** 8798
[18] Jiang S, Li L, Wang Z, Mak K F and Shan J 2018 *Nat. Nanotechnol.* **13** 549
[19] Leutenantsmeyer J C, Kaverzin A A, Wojtaszek M and Wees B J V 2016 *2D Mater.* **4** 014001
[20] Huang B, Clark G, Navarro-Moratalla E, Klein D R, Cheng R, Seyler K L, Zhong D, Schmidgall E, McGuire M A, Cobden D H, Yao W, Xiao D, Jarillo-Herrero P and Xu X 2017 *Nature* **546** 270
[21] Gong C, Li L, Li Z, Ji H, Stern A, Xia Y, Cao T, Bao W, Wang C, Wang Y, Qiu Z Q, Cava R J, Louie S G, Xia J and Zhang X 2017 *Nature* **546** 265
[22] Yao Y, Zhan X, Sendeku M G, Yu P, Dajan F T, Zhu C, Li N, Wang J, Wang F, Wang Z and He J 2021 *Nanotechnology* **32** 472001

[23] Cortie D L, Causer G L, Rule K C, Fritzsche H, Kreuzpaintner W and Klose F 2020 *Adv. Funct. Mater.* **30** 1901414
[24] Onsager L 1944 *Phys. Rev.* **65** 117
[25] Mermin N D and Wagner H 1966 *Phys. Rev. Lett.* **17** 1133
[26] Lines M E 1967 *Phys. Lett. A* **24** 591
[27] Lines M E 1969 *J. Appl. Phys.* **40** 1352
[28] Elmers H J 1995 *Int. J. Mod. Phys. B* **9** 3115
[29] Kohlhepp J, Elmers H J, Cordes S and Gradmann U 1992 *Phys. Rev. B* **45** 12287
[30] Vaz C A F, Bland J A C and Lauhoff G 2008 *Rep. Prog. Phys.* **71** 056501
[31] Yang S, Zhang T and Jiang C 2021 *Adv. Sci.* **8** 2002488
[32] Huang B, McGuire M A, May A F, Xiao D, Jarillo-Herrero P and Xu X 2020 *Nat. Mater.* **19** 1276
[33] Novoselov K S, Geim A K, Morozov S V, Jiang D, Zhang Y, Dubonos S V, Grigorieva I V and Firsov A A 2004 *Science* **306** 666
[34] Xu X, Yao W, Xiao D and Heinz T F 2014 *Nat. Phys.* **10** 343
[35] Cheng R, Li D, Zhou H, Wang C, Yin A, Jiang S, Liu Y, Chen Y, Huang Y and Duan X 2014 *Nano Lett.* **14** 5590
[36] Avsar A, Ciarrocchi A, Pizzochero M, Unuchek D, Yazyev O V and Kis A 2019 *Nat. Nanotechnol.* **14** 674
[37] Červenka J, Katsnelson M I and Flipse C F J 2009 *Nat. Phys.* **5** 840
[38] Ge J, Luo T, Lin Z, Shi J, Liu Y, Wang P, Zhang Y, Duan W and Wang J 2021 *Adv. Mater.* **33** 2005465
[39] Blonski P, Tucek J, Sofer Z, Mazánek V, Petr M, Pumera M, Otyepka M and Zboril R 2017 *J. Am. Chem. Soc.* **139** 3171
[40] Zhao C, Xu Z, Wang H, Wei J, Wang W, Bai X and Wang E 2014 *Adv. Funct. Mater.* **24** 5985
[41] Fan M, Wu J, Yuan J, Deng L, Zhong N, He L, Cui J, Wang Z, Behera S K, Zhang C, Lai J, Jawdat B I, Vajtai R, Deb P, Huang Y, Qian J, Yang J, Tour J M, Lou J, Chu C W, Sun D and Ajayan P M 2019 *Adv. Mater.* **31** 1805778
[42] Tuček J, Holá K, Zoppellaro G, Błoński P, Langer R, Medved' M, Susi T, Otyepka M and Zbořil R 2018 *ACS Nano* **12** 12847
[43] Wang X, Du K, Fredrik Liu Y Y, Hu P, Zhang J, Zhang Q, Owen M H S, Lu X, Gan C K, Sengupta P, Kloc C and Xiong Q 2016 *2D Mater.* **3** 031009
[44] Lee J U, Lee S, Ryoo J H, Kang S, Kim T Y, Kim P, Park C H, Park J G and Cheong H 2016 *Nano Lett.* **16** 7433
[45] Irkhin V Y and Katanin A A 1999 *Phys. Rev. B* **60** 2990
[46] Burch K S, Mandrus D and Park J G 2018 *Nature* **563** 47
[47] Zhong D, Seyler K L, Linpeng X, Cheng R, Sivadas N, Huang B, Schmidgall E, Taniguchi T, Watanabe K, McGuire M A, Yao W, Xiao D, Fu K M C and Xu X 2017 *Sci. Adv.* **3** e1603113
[48] Kitaev A 2006 *Ann. Phys.* **321** 2
[49] Jackeli G and Khaliullin G 2009 *Phys. Rev. Lett.* **102** 017205
[50] Banerjee A, Yan J, Knolle J, Bridges C A, Stone M B, Lumsden M D, Mandrus D G, Tennant D A, Moessner R and Nagler S E 2017 *Science* **356** 1055
[51] Huang C J, Liu J Q and Chen G 2021 arXiv: 2105.02673v1 [cond-mat.str-el]
[52] Duong D L, Yun S J and Lee Y H 2017 *ACS Nano* **11** 11803
[53] McGuire M A 2017 *Crystals* **7** 121
[54] Mounet N, Gibertini M, Schwaller P, Campi D, Merkys A, Marrazzo A, Sohier T, Castelli I E, Cepellotti A, Pizzi G and Marzari N 2018 *Nat. Nanotechnol.* **13** 246
[55] Su J, Liu K, Wang F, Jin B, Guo Y, Liu G, Li H and Zhai T 2019 *Adv. Mater. Interfaces* **6** 1900741
[56] McGuire M A 2020 *J. Appl. Phys.* **128** 110901
[57] Liu Y, Zhang S, He J, Wang Z M and Liu Z 2019 *Nano-Micro Lett.* **11** 13
[58] Huang P, Zhang P, Xu S, Wang H, Zhang X and Zhang H 2020 *Nanoscale* **12** 2309
[59] May A F, Yan J and McGuire M A 2020 *J. Appl. Phys.* **128** 051101
[60] Blei M, Lado J L, Song Q, Dey D, Erten O, Pardo V, Comin R, Tongay S and Botana A S 2021 *Appl. Phys. Rev.* **8** 021301
[61] Och M, Martin M B, Dlubak B, Seneor P and Mattevi C 2021 *Nanoscale* **13** 2157
[62] Jiang X, Liu Q, Xing J, Liu N, Guo Y, Liu Z and Zhao J 2021 *Appl. Phys. Rev.* **8** 031305
[63] Ningrum V P, Liu B, Wang W, Yin Y, Cao Y, Zha C, Xie H, Jiang X, Sun Y and Qin S 2020 *Research* **2020** 1768918
[64] Zhang W, Wong P K J, Zhu R and Wee A T S 2019 *InfoMat* **1** 479
[65] Zhang H X, Feng J, Wu H, Yu G and Han X 2021 *Chin. Phys. B* **30** 118504
[66] Jiang S, Li L, Wang Z, Shan J and Mak K F 2019 *Nat. Electron.* **2** 159
[67] Butler S Z, Hollen S M, Cao L, Cui Y, Gupta J A, Gutiérrez H R, Heinz T F, Hong S S, Huang J, Ismach A F, Johnston-Halperin E, Kuno M, Plashnitsa V V, Robinson R D, Ruoff R S, Salahuddin S, Shan J, Shi L, Spencer M G, Terrones M, Windl W and Goldberger J E 2013 *ACS Nano* **7** 2898
[68] Okuma R, Ritter C, Nilsen G J and Okada Y 2021 *Phys. Rev. Mater.* **5** L121401
[69] Tian C, Pan F, Wang L, Ye D, Sheng J, Wang J, Liu J, Huang J, Zhang H, Xu D, Qin J, Hao L, Xia Y, Li H, Tong X, Wu L, Chen J H, Jia S, Cheng P, Yang J and Zheng Y 2021 *Phys. Rev. B* **104** 214410
[70] Rau J G, Lee E K H and Kee H Y 2014 *Phys. Rev. Lett.* **112** 077204
[71] Dzyaloshinsky I 1958 *J. Phys. Chem. Solids* **4** 241
[72] Zhang H, Chen R, Zhai K, Chen X, Caretta L, Huang X, Chopdekar R V, Cao J, Sun J, Yao J, Birgeneau R and Ramesh R 2020 *Phys. Rev. B* **102** 064417
[73] Seo J, Kim D Y, An E S, Kim K, Kim G Y, Hwang S Y, Kim D W, Jang B G, Kim H, Eom G, Seo S Y, Stania R, Muntwiler M, Lee J, Watanabe K, Taniguchi T, Jo Y J, Lee J, Min B I, Jo M H, Yeom H W, Choi S Y, Shim J H and Kim J S 2020 *Sci. Adv.* **6** eaay8912
[74] Morosan E, Zandbergen H W, Li L, Lee M, Checkelsky J G, Heinrich M, Siegrist T, Ong N P and Cava R J 2007 *Phys. Rev. B* **75** 104401
[75] Su J, Wang M, Liu G, Li H, Han J and Zhai T 2020 *Adv. Sci.* **7** 2001722
[76] McGuire M A, Dixit H, Cooper V R and Sales B C 2015 *Chem. Mater.* **27** 612
[77] Carteaux V, Brunet D, Ouvrard G and Andre G 1995 *J. Phys.: Condens. Matter* **7** 69
[78] Kim H H, Yang B, Li S, Jiang S, Jin C, Tao Z, Nichols G, Sfigakis F, Zhong S, Li C, Tian S, Cory D G, Miao G X, Shan J, Mak K F, Lei H, Sun K, Zhao L and Tsen A W 2019 *PNAS* **116** 11131
[79] Tian S, Zhang J F, Li C, Ying T, Li S, Zhang X, Liu K and Lei H 2019 *J. Am. Chem. Soc.* **141** 5326
[80] Son S, Coak M J, Lee N, Kim J, Kim T Y, Hamidov H, Cho H, Liu C, Jarvis D M, Brown P A C, Kim J H, Park C H, Khomskii D I, Saxena S S and Park J G 2019 *Phys. Rev. B* **99** 041402
[81] Kong T, Stolze K, Timmons E I, Tao J, Ni D, Guo S, Yang Z, Prozorov R and Cava R J 2019 *Adv. Mater.* **31** 1808074
[82] Peng Y, Cheng X, Gu P, Wang F, Yang J, Xue M, Yang W, Wang C, Liu S, Watanabe K, Taniguchi T, Ye Y and Yang J 2020 *Adv. Funct. Mater.* **30** 1910036
[83] Bonilla M, Kolekar S, Ma Y, Diaz H C, Kalappattil V, Das R, Eggers T, Gutierrez H R, Phan M H and Batzill M 2018 *Nat. Nanotechnol.* **13** 289
[84] Jiang S, Shan J and Mak K F 2018 *Nat. Mater.* **17** 406
[85] Wu J, Liu F, Sasase M, Ienaga K, Obata Y, Yukawa R, Horiba K, Kumigashira H, Okuma S, Inoshita T and Hosono H 2019 *Sci. Adv.* **5** eaax9989
[86] Otrokov M M, Klimovskikh I I, Bentmann H, Estyunin D, Zeugner A, Aliev Z S, Gaß S, Wolter A U B, Koroleva A V, Shikin A M, Blanco-Rey M, Hoffmann M, Rusinov I P, Vyazovskaya A Y, Eremeev S V, Koroteev Y M, Kuznetsov V M, Freyse F, Sánchez-Barriga J, Amiraslanov I R, Babanly M B, Mamedov N T, Abdullayev N A, Zverev V N, Alfonsov A, Kataev V, Büchner B, Schwier E F, Kumar S, Kimura A, Petaccia L, Di Santo G, Vidal R C, Schatz S, Kißner K, Ünzelmann M, Min C H, Moser S, Peixoto T R F, Reinert F, Ernst A, Echenique P M, Isaeva A and Chulkov E V 2019 *Nature* **576** 416
[87] Sass P M, Kim J, Vanderbilt D, Yan J and Wu W 2020 *Phys. Rev. Lett.* **125** 037201
[88] Li H, Liu S, Liu C, Zhang J, Xu Y, Yu R, Wu Y, Zhang Y and Fan S 2020 *Phys. Chem. Chem. Phys.* **22** 556
[89] Klimovskikh I I, Otrokov M M, Estyunin D, Eremeev S V, Filnov S O, Koroleva A, Shevchenko E, Voroshnin V, Rybkin A G, Rusinov I P, Blanco-Rey M, Hoffmann M, Aliev Z S, Babanly M B, Amiraslanov I R, Abdullayev N A, Zverev V N, Kimura A, Tereshchenko O E, Kokh K A, Petaccia L, Di Santo G, Ernst A, Echenique P M, Mamedov N T, Shikin A M and Chulkov E V 2020 *npj Quantum Mater.* **5** 54
[90] Yan J Q, Zhang Q, Heitmann T, Huang Z, Chen K Y, Cheng J G, Wu W, Vaknin D, Sales B C and McQueeney R J 2019 *Phys. Rev. Mater.* **3** 064202

[91] Yan J Q, Liu Y H, Parker D S, Wu Y, Aczel A A, Matsuda M, McGuire M A and Sales B C 2020 *Phys. Rev. Mater.* **4** 054202

[92] Hu C, Gordon K N, Liu P, Liu J, Zhou X, Hao P, Narayan D, Emmanouilidou E, Sun H, Liu Y, Brawer H, Ramirez A P, Ding L, Cao H, Liu Q, Dessau D and Ni N 2020 *Nat. Commun.* **11** 97

[93] Tian S, Gao S, Nie S, Qian Y, Gong C, Fu Y, Li H, Fan W, Zhang P, Kondo T, Shin S, Adell J, Fedderwitz H, Ding H, Wang Z, Qian T and Lei H 2020 *Phys. Rev. B* **102** 035144

[94] Otrokov M M, Rusinov I P, Blanco-Rey M, Hoffmann M, Vyazovskaya A Y, Eremeev S V, Ernst A, Echenique P M, Arnau A and Chulkov E V 2019 *Phys. Rev. Lett.* **122** 107202

[95] Li J, Li Y, Du S, Wang Z, Gu B L, Zhang S C, He K, Duan W and Xu Y 2019 *Sci. Adv.* **5** eaaw5685

[96] Calder S, Haglund A V, Liu Y, Pajerowski D M, Cao H B, Williams T J, Garlea V O and Mandrus D 2020 *Phys. Rev. B* **102** 024408

[97] Peng Y, Ding S, Cheng M, Hu Q, Yang J, Wang F, Xue M, Liu Z, Lin Z, Avdeev M, Hou Y, Yang W, Zheng Y and Yang J 2020 *Adv. Mater.* **32** 2001200

[98] Wildes A R, Simonet V, Ressouche E, Ballou R and McIntyre G J 2017 *J. Phys.: Condens. Matter* **29** 455801

[99] Kim K, Lim S Y, Lee J U, Lee S, Kim T Y, Park K, Jeon G S, Park C H, Park J G and Cheong H 2019 *Nat. Commun.* **10** 345

[100] Kuo C T, Neumann M, Balamurugan K, Park H J, Kang S, Shiu H W, Kang J H, Hong B H, Han M, Noh T W and Park J G 2016 *Sci. Rep.* **6** 20904

[101] Ressouche E, Loire M, Simonet V, Ballou R, Stunault A and Wildes A 2010 *Phys. Rev. B* **82** 100408

[102] Kim K, Lim S Y, Kim J, Lee J U, Lee S, Kim P, Park K, Son S, Park C H, Park J G and Cheong H 2019 *2D Mater.* **6** 041001

[103] Sun Y J, Tan Q H, Liu X L, Gao Y F and Zhang J 2019 *J. Phys. Chem. Lett.* **10** 3087

[104] Long G, Henck H, Gibertini M, Dumcenco D, Wang Z, Taniguchi T, Watanabe K, Giannini E and Morpurgo A F 2020 *Nano Lett.* **20** 2452

[105] Hwang S R, Li W H, Lee K C, Lynn J W and Wu C G 2000 *Phys. Rev. B* **62** 14157

[106] Cable J W, Wilkinson M K, Wollan E O and Koehler W C 1962 *Phys. Rev.* **127** 714

[107] Jacobs I S and Lawrence P E 1967 *Phys. Rev.* **164** 866

[108] Kurumaji T, Seki S, Ishiwata S, Murakawa H, Tokunaga Y, Kaneko Y and Tokura Y 2011 *Phys. Rev. Lett.* **106** 167206

[109] Kurumaji T, Seki S, Ishiwata S, Murakawa H, Kaneko Y and Tokura Y 2013 *Phys. Rev. B* **87** 014429

[110] Ju H, Lee Y, Kim K T, Choi I H, Roh C J, Son S, Park P, Kim J H, Jung T S, Kim J H, Kim K H, Park J G and Lee J S 2021 *Nano Lett.* **21** 5126

[111] Kadowaki H, Ubukoshi K, Hirakawa K, Martínez J L and Shirane G 1987 *J. Phys. Soc. Jpn.* **56** 4027

[112] Hirakawa K, Kadowaki H and Ubukoshi K 1983 *J. Phys. Soc. Jpn.* **52** 1814

[113] Liang J, Wang W, Du H, Hallal A, Garcia K, Chshiev M, Fert A and Yang H 2020 *Phys. Rev. B* **101** 184401

[114] Yuan J, Yang Y, Cai Y, Wu Y, Chen Y, Yan X and Shen L 2020 *Phys. Rev. B* **101** 094420

[115] Zhou J, Feng Y P and Shen L 2020 *Phys. Rev. B* **102** 180407

[116] Zhao P, Ma Y, Lei C, Wang H, Huang B and Dai Y 2019 *Appl. Phys. Lett.* **115** 261605

[117] Grönke M, Buschbeck B, Schmidt P, Valldor M, Oswald S, Hao Q, Lubk A, Wolf D, Steiner U, Büchner B and Hampel S 2019 *Adv. Mater. Interfaces* **6** 1901410

[118] Nguyen G D, Lee J, Berlijn T, Zou Q, Hus S M, Park J, Gai Z, Lee C and Li A P 2018 *Phys. Rev. B* **97** 014425

[119] Li Q, Yang M, Gong C, Chopdekar R V, N'Diaye A T, Turner J, Chen G, Scholl A, Shafer P, Arenholz E, Schmid A K, Wang S, Liu K, Gao N, Admasu A S, Cheong S W, Hwang C, Li J, Wang F, Zhang X and Qiu Z 2018 *Nano Lett.* **18** 5974

[120] Tan C, Lee J, Jung S G, Park T, Albarakati S, Partridge J, Field M R, McCulloch D G, Wang L and Lee C 2018 *Nat. Commun.* **9** 1554

[121] Gao Y, Yan S, Yin Q, Huang H, Li Z, Zhu Z, Cai J, Shen B, Lei H, Zhang Y and Wang S 2022 *Phys. Rev. B* **105** 014426

[122] Liu Q, Wang L, Fu Y, Zhang X, Huang L, Su H, Lin J, Chen X, Yu D, Cui X, Mei J W and Dai J F 2021 *Phys. Rev. B* **103** 235411

[123] Gu P, Sun Y, Wang C, Peng Y, Zhu Y, Cheng X, Yuan K, Lyu C, Liu X, Tan Q, Zhang Q, Gu L, Wang Z, Wang H, Han Z, Watanabe K, Taniguchi T, Yang J, Zhang J, Ji W, Tan P H and Ye Y 2022 *Nano Lett.* **22** 1233

[124] Zeng Y, Gu P, Zhao Z, Zhang B, Lin Z, Peng Y, Li W, Zhao W, Leng Y, Tan P, Yang T, Zhang Z, Song Y, Yang J, Ye Y, Tian K and Hou Y 2022 *Adv. Mater.* **34** 2108847

[125] Ghimire N J, Botana A S, Jiang J S, Zhang J, Chen Y S and Mitchell J F 2018 *Nat. Commun.* **9** 3280

[126] Niu Q, Zhang W, Chan Y T, O'Farrell E C T, Doganov R, Yip K Y, Lai K T, Yu W C, Özyilmaz B, Stewart G R, Kim J S and Goh S K 2020 *Phys. Rev. Res.* **2** 023297

[127] Pawula F, Daou R, Hébert S, Lebedev O, Maignan A, Subedi A, Kakefuda Y, Kawamoto N, Baba T and Mori T 2019 *Phys. Rev. B* **99** 085422

[128] Binnewies M, Schmidt M and Schmidt P 2017 *Z. Anorg. Allg. Chem.* **643** 1295

[129] Selter S, Shemerliuk Y, Büchner B and Aswartham S 2021 *Crystals* **11** 500

[130] Taylor B, Steger J, Wold A and Kostiner E 1974 *Inorg. Chem.* **13** 2719

[131] Ji H, Stokes R A, Alegria L D, Blomberg E C, Tanatar M A, Reijnders A, Schoop L M, Liang T, Prozorov R, Burch K S, Ong N P, Petta J R and Cava R J 2013 *J. Appl. Phys.* **114** 114907

[132] Lin G T, Zhuang H L, Luo X, Liu B J, Chen F C, Yan J, Sun Y, Zhou J, Lu W J, Tong P, Sheng Z G, Qu Z, Song W H, Zhu X B and Sun Y P 2017 *Phys. Rev. B* **95** 245212

[133] May A F, Calder S, Cantoni C, Cao H and McGuire M A 2016 *Phys. Rev. B* **93** 014411

[134] Yu W, Li J, Herng T S, Wang Z, Zhao X, Chi X, Fu W, Abdelwahab I, Zhou J, Dan J, Chen Z, Chen Z, Li Z, Lu J, Pennycook S J, Feng Y P, Ding J and Loh K P 2019 *Adv. Mater.* **31** 1903779

[135] Wang N, Tang H, Shi M, Zhang H, Zhuo W, Liu D, Meng F, Ma L, Ying J and Zou L 2019 *J. Am. Chem. Soc.* **141** 17166

[136] Meng L, Zhou Z, Xu M, Yang S, Si K, Liu L, Wang X, Jiang H, Li B, Qin P, Zhang P, Wang J, Liu Z, Tang P, Ye Y, Zhou W, Bao L, Gao H J and Gong Y 2021 *Nat. Commun.* **12** 809

[137] Xian J J, Wang C, Nie J H, Li R, Han M, Lin J, Zhang W H, Liu Z Y, Zhang Z M, Miao M P, Yi Y, Wu S, Chen X, Han J, Xia Z, Ji W and Fu Y S 2022 *Nat. Commun.* **13** 257

[138] Wang C, Wu X, Ma Y, Mu G, Li Y, Luo C, Xu H, Zhang Y, Yang J, Tang X, Zhang J, Bao W and Duan C 2018 *J. Mater. Chem. A* **6** 8299

[139] Rajan A, Underwood K, Mazzola F and King P D C 2020 *Phys. Rev. Mater.* **4** 014003

[140] Lohmann M, Su T, Niu B, Hou Y, Alghamdi M, Aldosary M, Xing W, Zhong J, Jia S, Han W, Wu R, Cui Y T and Shi J 2019 *Nano Lett.* **19** 2397

[141] Karpiak B, Cummings A W, Zollner K, Vila M, Khokhriakov D, Hoque A M, Dankert A, Svedlindh P, Fabian J, Roche S and Dash S P 2019 *2D Materials* **7** 015026

[142] Ostwal V, Shen T and Appenzeller J 2020 *Adv. Mater.* **32** 1906021

[143] Mogi M, Yasuda K, Fujimura R, Yoshimi R, Ogawa N, Tsukazaki A, Kawamura M, Takahashi K S, Kawasaki M and Tokura Y 2021 *Nat. Commun.* **12** 1404

[144] Wang Z, Zhang T, Ding M, Dong B, Li Y, Chen M, Li X, Huang J, Wang H, Zhao X, Li Y, Li D, Jia C, Sun L, Guo H, Ye Y, Sun D, Chen Y, Yang T, Zhang J, Ono S, Han Z and Zhang Z 2018 *Nat. Nanotechnol.* **13** 554

[145] Idzuchi H, Allcca A E L, Pan X C, Tanigaki K and Chen Y P 2019 *Appl. Phys. Lett.* **115** 232403

[146] O'Hara D J, Zhu T, Trout A H, Ahmed A S, Luo Y K, Lee C H, Brenner M R, Rajan S, Gupta J A, McComb D W and Kawakami R K 2018 *Nano Lett.* **18** 3125

[147] Zhang X, Lu Q, Liu W, Niu W, Sun J, Cook J, Vaninger M, Miceli P F, Singh D J, Lian S W, Chang T R, He X, Du J, He L, Zhang R, Bian G and Xu Y 2021 *Nat. Commun.* **12** 2492

[148] Kim D, Lee C, Jang B G, Kim K and Shim J H 2021 *Sci. Rep.* **11** 17567

[149] Duvjir G, Choi B K, Jang I, Ulstrup S, Kang S, Thi Ly T, Kim S, Choi Y H, Jozwiak C, Bostwick A, Rotenberg E, Park J G, Sankar R, Kim K S, Kim J and Chang Y J 2018 *Nano Lett.* **18** 5432

[150] Li F, Tu K and Chen Z 2014 *J. Phys. Chem. C* **118** 21264

[151] Pushkarev G V, Mazurenko V G, Mazurenko V V and Boukhvalov D W 2019 *Phys. Chem. Chem. Phys.* **21** 22647

[152] Sumida K, Takeda Y, Kusaka S, Kobayashi K and Hirahara T 2022 *Phys. Rev. Mater.* **6** 014006

[153] Feng J, Biswas D, Rajan A, Watson M D, Mazzola F, Clark O J, Underwood K, Marković I, McLaren M, Hunter A, Burn D M, Duffy L B, Barua S, Balakrishnan G, Bertran F, Le Fèvre P, Kim T K, van der Laan G, Hesjedal T, Wahl P and King P D C 2018 *Nano Lett.* **18** 4493

[154] Wong P K J, Zhang W, Bussolotti F, Yin X, Herng T S, Zhang L, Huang Y L, Vinai G, Krishnamurthi S, Bukhvalov D W, Zheng Y J, Chua R, N'Diaye A T, Morton S A, Yang C Y, Ou Yang K H, Torelli P, Chen W, Goh K E J, Ding J, Lin M T, Brocks G, de Jong M P, Castro Neto A H and Wee A T S 2019 *Adv. Mater.* **31** 1901185

[155] Fumega A O, Gobbi M, Dreher P, Wan W, González-Orellana C, Peña-Díaz M, Rogero C, Herrero-Martín J, Gargiani P, Ilyn M, Ugeda M M, Pardo V and Blanco-Canosa S 2019 *J. Phys. Chem. C* **123** 27802

[156] Coelho P M, Nguyen Cong K, Bonilla M, Kolekar S, Phan M H, Avila J, Asensio M C, Oleynik I I and Batzill M 2019 *J. Phys. Chem. C* **123** 14089

[157] Wang X, Li D, Li Z, Wu C, Che C M, Chen G and Cui X 2021 *ACS Nano* **15** 16236

[158] Freitas D C, Weht R, Sulpice A, Remenyi G, Strobel P, Gay F, Marcus J and Nunez-Regueiro M 2015 *J. Phys.: Condens. Matter* **27** 176002

[159] Sun X, Li W, Wang X, Sui Q, Zhang T, Wang Z, Liu L, Li D, Feng S, Zhong S, Wang H, Bouchiat V, Nunez Regueiro M, Rougemaille N, Coraux J, Purbawati A, Hadj-Azzem A, Wang Z, Dong B, Wu X, Yang T, Yu G, Wang B, Han Z, Han X and Zhang Z 2020 *Nano Research* **13** 3358

[160] Huang M, Wang S, Wang Z, Liu P, Xiang J, Feng C, Wang X, Zhang Z, Wen Z, Xu H, Yu G, Lu Y, Zhao W, Yang S A, Hou D and Xiang B 2021 *ACS Nano* **15** 9759

[161] Zhang X, Ambhire S C, Lu Q, Niu W, Cook J, Jiang J S, Hong D, Alahmed L, He L, Zhang R, Xu Y, Zhang S S L, Li P and Bian G 2021 *ACS Nano* **15** 15710

[162] Deiseroth H J, Aleksandrov K, Reiner C, Kienle L and Kremer R K 2006 *Eur. J. Inorg. Chem.* **2006** 1561

[163] May A F, Ovchinnikov D, Zheng Q, Hermann R, Calder S, Huang B, Fei Z, Liu Y, Xu X and McGuire M A 2019 *ACS Nano* **13** 4436

[164] Stahl J, Shlaen E and Johrendt D 2018 *Z. Anorg. Allg. Chem.* **644** 1923

[165] Seo J, An E S, Park T, Hwang S Y, Kim G Y, Song K, Noh W s, Kim J Y, Choi G S, Choi M, Oh E, Watanabe K, Taniguchi T, Park J H, Jo Y J, Yeom H W, Choi S Y, Shim J H and Kim J S 2021 *Nat. Commun.* **12** 2844

[166] Fei Z, Huang B, Malinowski P, Wang W, Song T, Sanchez J, Yao W, Xiao D, Zhu X, May A F, Wu W, Cobden D H, Chu J H and Xu X 2018 *Nat. Mater.* **17** 778

[167] May A F, Bridges C A and McGuire M A 2019 *Phys. Rev. Mater.* **3** 104401

[168] Ribeiro M, Gentile G, Marty A, Dosenovic D, Okuno H, Vergnaud C, Jacquot J F, Jalabert D, Longo D, Ohresser P, Hallal A, Chshiev M, Boulle O, Bonell F and Jamet M 2022 *npj 2D Mater. Appl.* **6** 10

[169] Ohta T, Sakai K, Taniguchi H, Driesen B, Okada Y, Kobayashi K and Niimi Y 2020 *Appl. Phys. Express* **13** 043005

[170] Kim K, Seo J, Lee E, Ko K T, Kim B S, Jang B G, Ok J M, Lee J, Jo Y J, Kang W, Shim J H, Kim C, Yeom H W, Il Min B, Yang B J and Kim J S 2018 *Nat. Mater.* **17** 794

[171] You Y R, aGong Y, Li H, Li Z F, Zhu M M, Tang J X, Liu E K, Yao Y, Xu G Z, Xu F and Wang W H 2019 *Phys. Rev. B* **100** 134441

[172] Wang H, Wang C, Li Z A, Tian H, Shi Y, Yang H and Li J 2020 *Appl. Phys. Lett.* **116** 192403

[173] Ding B, Li Z, Xu G, Li H, Hou Z, Liu E, Xi X, Xu F, Yao Y and Wang W 2020 *Nano Lett.* **20** 868

[174] Park T E, Peng L, Liang J, Hallal A, Yasin F S, Zhang X, Song K M, Kim S J, Kim K, Weigand M, Schütz G, Finizio S, Raabe J, Garcia K, Xia J, Zhou Y, Ezawa M, Liu X, Chang J, Koo H C, Kim Y D, Chshiev M, Fert A, Yang H, Yu X and Woo S 2021 *Phys. Rev. B* **103** 104410

[175] Wu Y, Zhang S, Zhang J, Wang W, Zhu Y L, Hu J, Yin G, Wong K, Fang C, Wan C, Han X, Shao Q, Taniguchi T, Watanabe K, Zang J, Mao Z, Zhang X and Wang K L 2020 *Nat. Commun.* **11** 3860

[176] Yang M, Li Q, Chopdekar R V, Dhall R, Turner J, Carlström J D, Ophus C, Klewe C, Shafer P, N'Diaye A T, Choi J W, Chen G, Wu Y Z, Hwang C, Wang F and Qiu Z Q 2020 *Sci. Adv.* **6** eabb5157

[177] Deng Y, Yu Y, Song Y, Zhang J, Wang N Z, Sun Z, Yi Y, Wu Y Z, Wu S, Zhu J, Wang J, Chen X H and Zhang Y 2018 *Nature* **563** 94

[178] Wang Y, Wang C, Liang S J, Ma Z, Xu K, Liu X, Zhang L, Admasu A S, Cheong S W, Wang L, Chen M, Liu Z, Cheng B, Ji W and Miao F 2020 *Adv. Mater.* **32** 2004533

[179] Zhang K, Han S, Lee Y, Coak M J, Kim J, Hwang I, Son S, Shin J, Lim M, Jo D, Kim K, Kim D, Lee H W and Park J G 2021 *Adv. Mater.* **33** 2004110

[180] Lin H, Yan F, Hu C, Zheng Y, Sheng Y, Zhu W, Wang Z, Zheng H and Wang K 2022 *Nanoscale* **14** 2352

[181] Wang X, Li Z, Zhang M, Hou T, Zhao J, Li L, Rahman A, Xu Z, Gong J, Chi Z, Dai R, Wang Z, Qiao Z and Zhang Z 2019 *Phys. Rev. B* **100** 014407

[182] Ding S, Liang Z, Yang J, Yun C, Zhang P, Li Z, Xue M, Liu Z, Tian G, Liu F, Wang W, Yang W and Yang J 2021 *Phys. Rev. B* **103** 094429

[183] Xu X, Yang S, Wang H, Guzman R, Zhu Y, Peng Y, Zang Z, Xi M, Tian S and Li Y 2022 arXiv: 2204.09420 [cond-mat.mtrl-sci]

[184] Zheng G, Xie W Q, Albarakati S, Algarni M, Tan C, Wang Y, Peng J, Partridge J, Farrar L, Yi J, Xiong Y, Tian M, Zhao Y J and Wang L 2020 *Phys. Rev. Lett.* **125** 047202

[185] Zhang L, Huang X, Dai H, Wang M, Cheng H, Tong L, Li Z, Han X, Wang X, Ye L and Han J 2020 *Adv. Mater.* **32** 2002032

[186] Hu G, Zhu Y, Xiang J, Yang T Y, Huang M, Wang Z, Wang Z, Liu P, Zhang Y, Feng C, Hou D, Zhu W, Gu M, Hsu C H, Chuang F C, Lu Y, Xiang B and Chueh Y L 2020 *ACS Nano* **14** 12037

[187] Dai H, Cheng H, Cai M, Hao Q, Xing Y, Chen H, Chen X, Wang X and Han J B 2021 *ACS Appl. Mater. Interfaces* **13** 24314

[188] Zhang T, Zhang Y, Huang M, Li B, Sun Y, Qu Z, Duan X, Jiang C and Yang S 2022 *Adv. Sci.* **9** 2105483

[189] Zhu R, Zhang W, Shen W, Wong P K J, Wang Q, Liang Q, Tian Z, Zhai Y, Qiu C W and Wee A T S 2020 *Nano Lett.* **20** 5030

[190] Tian C K, Wang C, Ji W, Wang J C, Xia T L, Wang L, Liu J J, Zhang H X and Cheng P 2019 *Phys. Rev. B* **99** 184428

[191] Drachuck G, Salman Z, Masters M W, Taufour V, Lamichhane T N, Lin Q, Straszheim W E, Bud'ko S L and Canfield P C 2018 *Phys. Rev. B* **98** 144434

[192] Tian C, Pan F, Xu S, Ai K, Xia T and Cheng P 2020 *Appl. Phys. Lett.* **116** 202402

[193] May A F, Du M H, Cooper V R and McGuire M A 2020 *Phys. Rev. Mater.* **4** 074008

[194] Chen X, Shao Y T, Chen R, Susarla S, Hogan T, He Y, Zhang H, Wang S, Yao J and Ercius P 2022 arXiv: 2203.00125v1 [cond-mat.mtrl-sci]

[195] Miyazaki T and Tezuka N 1995 *J. Magn. Magn. Mater.* **151** 403

[196] Wang Z, Sapkota D, Taniguchi T, Watanabe K, Mandrus D and Morpurgo A F 2018 *Nano Lett.* **18** 4303

[197] Zhu W, Lin H, Yan F, Hu C, Wang Z, Zhao L, Deng Y, Kudrynskyi Z R, Zhou T, Kovalyuk Z D, Zheng Y, Patanè A, Žutić I, Li S, Zheng H and Wang K 2021 *Adv. Mater.* **33** 2104658

[198] Lin H, Yan F, Hu C, Lv Q, Zhu W, Wang Z, Wei Z, Chang K and Wang K 2020 *ACS Appl. Mater. Interfaces* **12** 43921

[199] Hu C, Yan F, Li Y and Wang K 2021 *Chin. Phys. B* **30** 97505

[200] Su Y, Li X, Zhu M, Zhang J, You L and Tsymbal E Y 2021 *Nano Lett.* **21** 175

[201] Hu C, Zhang D, Yan F, Li Y, Lv Q, Zhu W, Wei Z, Chang K and Wang K 2020 *Sci. Bull.* **65** 1072

[202] Albarakati S, Tan C, Chen Z J, Partridge J G, Zheng G, Farrar L, Mayes E L H, Field M R, Lee C, Wang Y, Xiong Y, Tian M, Xiang F, Hamilton A R, Tretiakov O A, Culcer D, Zhao Y J and Wang L 2019 *Sci. Adv.* **5** eaaw0409

[203] Wang X, Tang J, Xia X, He C, Zhang J, Liu Y, Wan C, Fang C, Guo C, Yang W, Guang Y, Zhang X, Xu H, Wei J, Liao M, Lu X, Feng J, Li X, Peng Y, Wei H, Yang R, Shi D, Zhang X, Han Z, Zhang Z, Zhang G, Yu G and Han X 2019 *Sci. Adv.* **5** eaaw8904

[204] Alghamdi M, Lohmann M, Li J, Jothi P R, Shao Q, Aldosary M, Su T, Fokwa B P T and Shi J 2019 *Nano Lett.* **19** 4400

[205] Chen X, Wang H, Liu H, Wang C, Wei G, Fang C, Wang H, Geng C, Liu S, Li P, Yu H, Zhao W, Miao J, Li Y, Wang L, Nie T, Zhao J and Wu X 2022 *Adv. Mater.* **34** 2106172

[206] Zhao B, Ngaloy R, Hoque A M, Karpiak B, Khokhriakov D and Dash S P 2021 arXiv: 2107.00310v1 [cond-mat.mes-hall]

[207] Cong X, Liu X L, Lin M L and Tan P H 2020 *npj 2D Mater. Appl.* **4** 13

[208] Sun Z, Yi Y, Song T, Clark G, Huang B, Shan Y, Wu S, Huang D, Gao C, Chen Z, McGuire M, Cao T, Xiao D, Liu W T, Yao W, Xu X and Wu S 2019 *Nature* **572** 497

[209] Chu H, Roh C J, Island J O, Li C, Lee S, Chen J, Park J G, Young A F, Lee J S and Hsieh D 2020 *Phys. Rev. Lett.* **124** 027601

[210] Ni Z, Haglund A V, Wang H, Xu B, Bernhard C, Mandrus D G, Qian X, Mele E J, Kane C L and Wu L 2021 *Nat. Nanotechnol.* **16** 782
[211] McGuire M A, Clark G, Kc S, Chance W M, Jellison G E, Cooper V R, Xu X and Sales B C 2017 *Phys. Rev. Mater.* **1** 014001
[212] Telford E J, Dismukes A H, Lee K, Cheng M, Wieteska A, Bartholomew A K, Chen Y S, Xu X, Pasupathy A N, Zhu X, Dean C R and Roy X 2020 *Adv. Mater.* **32** 2003240
[213] Wang Z, Gutierrez-Lezama I, Ubrig N, Kroner M, Gibertini M, Taniguchi T, Watanabe K, Imamoglu A, Giannini E and Morpurgo A F 2018 *Nat. Commun.* **9** 2516
[214] Niu B, Su T, Francisco B A, Ghosh S, Kargar F, Huang X, Lohmann M, Li J, Xu Y, Taniguchi T, Watanabe K, Wu D, Balandin A, Shi J and Cui Y T 2020 *Nano Lett.* **20** 553
[215] Li S, Ye Z, Luo X, Ye G, Kim H H, Yang B, Tian S, Li C, Lei H, Tsen A W, Sun K, He R and Zhao L 2020 *Phys. Rev. X* **10** 011075
[216] Lee S H, Zhu Y, Wang Y, Miao L, Pillsbury T, Yi H, Kempinger S, Hu J, Heikes C A, Quarterman P, Ratcliff W, Borchers J A, Zhang H, Ke X, Graf D, Alem N, Chang C Z, Samarth N and Mao Z 2019 *Phys. Rev. Res.* **1** 012011
[217] de Jongh L J and Miedema A R 1974 *Adv. Phys.* **23** 1
[218] Wang Z, Gibertini M, Dumcenco D, Taniguchi T, Watanabe K, Giannini E and Morpurgo A F 2019 *Nat. Nanotechnol.* **14** 1116
[219] Yang S, Xu X, Zhu Y, Niu R, Xu C, Peng Y, Cheng X, Jia X, Huang Y, Xu X, Lu J and Ye Y 2021 *Phys. Rev. X* **11** 011003
[220] Zang Z, Zhu Y, Xi M, Tian S, Wang T, Gu P, Peng Y, Yang S, Xu X, Li Y, Han B, Liu L, Wang Y, Gao P, Yang J, Lei H, Huang Y and Ye Y 2022 *Phys. Rev. Lett.* **128** 017201
[221] Bedoya-Pinto A, Ji J R, Pandeya A K, Gargiani P, Valvidares M, Sessi P, Taylor J M, Radu F, Chang K and Parkin S S P 2021 *Science* **374** 616
[222] Dupont M, Kvashnin Y O, Shiranzaei M, Fransson J, Laflorencie N and Kantian A 2021 *Phys. Rev. Lett.* **127** 037204
[223] Wu Y, Cui Q, Zhu M, Liu X, Wang Y, Zhang J, Zheng X, Shen J, Cui P, Yang H and Wang S 2021 *ACS Appl. Mater. Interfaces* **13** 10656
[224] Jiang D, Yuan T, Wu Y, Wei X, Mu G, An Z and Li W 2020 *ACS Appl. Mater. Interfaces* **12** 49252
[225] López-Paz S A, Guguchia Z, Pomjakushin V Y, Witteveen C, Cervellino A, Luetkens H, Casati N, Morpurgo A F and von Rohr F O 2022 arXiv: 2203.11785v1 [cond-mat.mtrl-sci]
[226] Lee K, Dismukes A H, Telford E J, Wiscons R A, Wang J, Xu X, Nuckolls C, Dean C R, Roy X and Zhu X 2021 *Nano Lett.* **21** 3511
[227] Telford E J, Dismukes A H, Dudley R L, Wiscons R A, Lee K, Yu J, Shabani S, Scheie A, Watanabe A, Taniguchi T, Xiao D, Pasupathy A N, Nuckolls C, Zhu X Y, Dean C R and Roy X 2021 arXiv: 2106.08471v1 [cond-mat.mes-hall]
[228] Wu F, Gutierrez-Lezama I, Lopez-Paz S A, Gibertini M, Watanabe K, Taniguchi T, von Rohr F O, Ubrig N and Morpurgo A F 2022 *Adv. Mater.* **34** 2109759
[229] Cenker J, Sivakumar S, Xie K, Miller A, Thijssen P, Liu Z, Dismukes A, Fonseca J, Anderson E, Zhu X, Roy X, Xiao D, Chu J H, Cao T and Xu X 2022 *Nat. Nanotechnol.* **17** 256
[230] Ghiasi T S, Kaverzin A A, Dismukes A H, de Wal D K, Roy X and van Wees B J 2021 *Nat. Nanotechnol.* **16** 788
[231] Zhuang H L and Zhou J 2016 *Phys. Rev. B* **94** 195307
[232] Pei Q L, Luo X, Lin G T, Song J Y, Hu L, Zou Y M, Yu L, Tong W, Song W H, Lu W J and Sun Y P 2016 *J. Appl. Phys.* **119** 043902
[233] Joe M, Lee H, Alyörük M M, Lee J, Kim S Y, Lee C and Lee J H 2017 *J. Phys.: Condens. Matter* **29** 405801
[234] Peng Y, Lin Z, Tian G, Yang J, Zhang P, Wang F, Gu P, Liu X, Wang C W, Avdeev M, Liu F, Zhou D, Han R, Shen P, Yang W, Liu S, Ye Y and Yang J 2021 *Adv. Funct. Mater.* **32** 2106592
[235] Lee J, Ko T Y, Kim J H, Bark H, Kang B, Jung S G, Park T, Lee Z, Ryu S and Lee C 2017 *ACS Nano* **11** 10935
[236] Gu P, Tan Q, Wan Y, Li Z, Peng Y, Lai J, Ma J, Yao X, Yang S, Yuan K, Sun D, Peng B, Zhang J and Ye Y 2020 *ACS Nano* **14** 1003
[237] Zhang H, Li Y, Hu X, Xu J, Chen L, Li G, Yin S, Chen J, Tan C, Kan X and Li L 2021 *Appl. Phys. Lett.* **119** 171102
[238] Bud'ko S L, Gati E, Slade T J and Canfield P C 2021 *Phys. Rev. B* **103** 224407
[239] Son J, Son S, Park P, Kim M, Tao Z, Oh J, Lee T, Lee S, Kim J, Zhang K, Cho K, Kamiyama T, Lee J H, Mak K F, Shan J, Kim M, Park J G and Lee J 2021 *ACS Nano* **15** 16904
[240] Yang J, Fang S, Peng Y, Liu S, Wu B, Quhe R, Ding S, Yang C, Ma J, Shi B, Xu L, Sun X, Tian G, Wang C, Shi J, Lu J and Yang J 2021 *Phys. Rev. Appl.* **16** 024011
[241] Wu R, Ross A, Ding S, Peng Y, He F, Ren Y, Lebrun R, Wu Y, Wang Z, Yang J, Brataas A and Kläui M 2021 arXiv: 2112.07306v1 [physics.app-ph]
[242] Son S, Shin Y J, Zhang K, Shin J, Lee S, Idzuchi H, Coak M J, Kim H, Kim J, Kim J H, Kim M, Kim D, Kim P and Park J G 2020 *2D Mater.* **7** 041005
[243] Shin J, Son S, Yun J, Park G, Zhang K, Shin Y J, Park J G and Kim D 2021 arXiv: 2111.05627v1 [cond-mat.supr-con]
[244] Ding S, Peng Y, Xue M, Liu Z, Liang Z, Yang W, Sun Y, Zhao J, Wang C, Liu S, Han J and Yang J 2020 *J. Phys.: Condens. Matter* **32** 405804
[245] Susner M A, Chyasnavichyus M, McGuire M A, Ganesh P and Maksymovych P 2017 *Adv. Mater.* **29** 1602852
[246] Wang F, Shifa T A, Yu P, He P, Liu Y, Wang F, Wang Z, Zhan X, Lou X, Xia F and He J 2018 *Adv. Funct. Mater.* **28** 1802151
[247] Cheng R, Okamoto S and Xiao D 2016 *Phys. Rev. Lett.* **117** 217202
[248] Shiomi Y, Takashima R and Saitoh E 2017 *Phys. Rev. B* **96** 134425
[249] Xing W, Qiu L, Wang X, Yao Y, Ma Y, Cai R, Jia S, Xie X C and Han W 2019 *Phys. Rev. X* **9** 011026
[250] Chen G, Qi S, Liu J, Chen D, Wang J, Yan S, Zhang Y, Cao S, Lu M, Tian S, Chen K, Yu P, Liu Z, Xie X C, Xiao J, Shindou R and Chen J H 2021 *Nat. Commun.* **12** 6279
[251] Ni Z, Zhang H, Hopper D A, Haglund A V, Huang N, Jariwala D, Bassett L C, Mandrus D G, Mele E J, Kane C L and Wu L 2021 *Phys. Rev. Lett.* **127** 187201
[252] Goossens D J 2010 *Eur. Phys. J. B* **78** 305
[253] Goossens D J, Wildes A R, Ritter C and Hicks T J 2000 *J. Phys.: Condens. Matter* **12** 1845
[254] Komarek A C, Taetz T, Fernández-Díaz M T, Trots D M, Möller A and Braden M 2009 *Phys. Rev. B* **79** 104425
[255] Zhang J, Wölfel A, Li L, van Smaalen S, Williamson H L and Kremer R K 2012 *Phys. Rev. B* **86** 134428
[256] Angelkort J, Wölfel A, Schönleber A, van Smaalen S and Kremer R K 2009 *Phys. Rev. B* **80** 144416
[257] Christensen A N, Johansson T and Quézel S 1975 *Acta Chem. Scand. Ser. A* **28** 1171
[258] Zhang T, Wang Y, Li H, Zhong F, Shi J, Wu M, Sun Z, Shen W, Wei B, Hu W, Liu X, Huang L, Hu C, Wang Z, Jiang C, Yang S, Zhang Q M and Qu Z 2019 *ACS Nano* **13** 11353
[259] Zhang M, Hu Q, Hua C, Cheng M, Liu Z, Song S, Wang F, He P, Cao G H and Xu Z A 2021 arXiv: 2108.02825v1 [cond-mat.str-el]
[260] Fernández-Rossier J 2019 *Science* **364** 935
[261] Song T, Sun Q C, Anderson E, Wang C, Qian J, Taniguchi T, Watanabe K, McGuire M A, Stöhr R, Xiao D, Cao T, Wrachtrup J and Xu X 2021 *Science* **374** 1140
[262] Cao Y, Fatemi V, Fang S, Watanabe K, Taniguchi T, Kaxiras E and Jarillo-Herrero P 2018 *Nature* **556** 43
[263] Xu Y, Ray A, Shao Y T, Jiang S, Lee K, Weber D, Goldberger J E, Watanabe K, Taniguchi T, Muller D A, Mak K F and Shan J 2022 *Nat. Nanotechnol.* **17** 143
[264] Xie H, Luo X, Ye G, Ye Z, Ge H, Sung S H, Rennich E, Yan S, Fu Y, Tian S, Lei H, Hovden R, Sun K, He R and Zhao L 2022 *Nat. Phys.* **18** 30
[265] Akram M, LaBollita H, Dey D, Kapeghian J, Erten O and Botana A S 2021 *Nano Lett.* **21** 6633
[266] Akram M and Erten O 2021 *Phys. Rev. B* **103** L140406